Green Chemistry

ROYAL SOCIETY OF CHEMISTRY

TUTORIAL REVIEW

View Article Online
View Journal | View Issue

Cite this: *Green Chem.*, 2024, **26**, 6318

Furfural production from lignocellulosic biomass: one-step and two-step strategies and techno-economic evaluation

Yuqi Bao,[a] Zicheng Du,[a] Xiaoying Liu,[a] Hui Liu,[a] Jinsong Tang,[a] Chengrong Qin,[a] Chen Liang,[a] Caoxing Huang[b] and Shuangquan Yao *[a]

Lignocellulosic biomass (LCB) is an abundant renewable energy resource. Hence, the conversion of biomass into fuel and platform chemicals has recently attracted considerable attention. Furfural is an important platform product that can be produced from xylan-rich lignocellulosic biomass. Hemicellulose undergoes two stages, hydrolysis and dehydration, resulting in the production of furfural. In this review, one-step and two-step strategies for furfural production and the subsequent techno-economic evaluation of the integration of furfural and other co-products are presented. The direct one-step production of furfural requires a one-time investment in severe pretreatment conditions or the use of more chemicals, whereas the two-step production requires the separation of additional prehydrolysates, followed by more drastic treatment conditions. In both strategies, water flow, steam flow, organic solvents, deep eutectic solvents (DESs) or ionic liquids (ILs) can be used as solvent phases to hydrolyze hemicellulose. Lewis acid and Brønsted acid catalysts can effectively convert hemicellulose-derived pentose into furfural. A biphasic solvent system can effectively prevent the degradation of furfural in water, thus increasing the yield and selectivity of furfural. The techno-economy assessment results indicate that biorefineries are transitioning to adopting an integrate model of co-production of furfural and other products. Alternative green approaches are increasingly being adopted to make the furfural industry more sustainable and profitable.

Received 21st February 2024,
Accepted 10th April 2024

DOI: 10.1039/d4gc00883a

rsc.li/greenchem

1. Introduction

The rapid depletion of non-renewable petroleum resources is driving the development of sustainable alternatives for the production of high energy density fuels and high value-added chemicals.[1] Non-edible and abundant lignocellulosic biomass materials are considered among the most promising feedstocks for the production of chemicals, fuels, and materials.[2] Biomass mainly consists of 40–60% cellulose, 20–40% hemicellulose, and 10–25% lignin along with minor extractives and minerals.[3] Therefore, the valorization of the three polymers into chemicals is critical for the efficient utilization of biomass and has recently received significant attention.[4] At least 30% of bulk chemicals is estimated to be derived from renewable biomass by 2050.[5]

However, the cell wall of cellulosic biomass is a cross-linked layered complex. Hence, it is necessary to break the anti-degradation barrier formed by the cross-linkages between lignin, cellulose, and hemicellulose.[6] Catalysts and solvents are critical for the effective depolymerization of the crosslinking bonds and for utilizing all the components. Hemicellulose, with the lowest degree of polymerization, can be separated first and hydrolyzed to form hemicellulose-derived sugars (xylo-oligosaccharides and xylose), which can be upgraded to furfural *via* dehydration. Hemicelluloses account for 20–30% of the total mass of three polymeric components of lignocellulosic biomass, among which hardwood, crop waste, and herbs are xylan-based polysaccharides.[7] Sugarcane bagasse and corncobs are responsible for 98% of all furfural production.[8] Approximately 140 billion tons of waste agricultural residues are generated annually worldwide and are potent candidates for furfural production.[9] Fig. 1 presents xylan-type hemicellulose resources and furfural applications.

Furfural has been identified as one of the top 12 platform chemicals and is mainly produced by the acid-catalyzed dehydration of hemicellulose-derived xylose.[10] It is a water-soluble, poisonous and flammable compound used as a pre-

[a]*Guangxi Key Laboratory of Clean Pulp & Papermaking and Pollution Control, School of Light Industrial and Food Engineering, Guangxi University, Nanning, 530004, PR China. E-mail: yaoshuangquan@gxu.edu.cn*
[b]*Jiangsu Co-Innovation Center of Efficient Processing and Utilization of Forest Resources, Nanjing Forestry University, Nanjing, 210037, PR China*

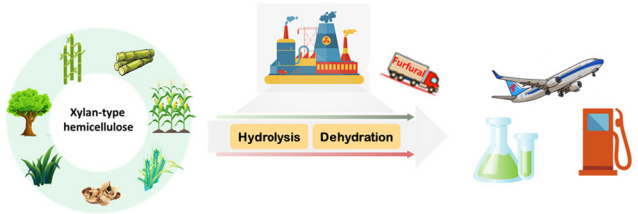

Fig. 1 Xylan-type hemicellulose resource and furfural applications.

cursor for fuels, solvents, and polymers in the fuel, pharmaceutical and plastic industries.[11] Furfural can be converted into a wide range of building blocks to replace fossil-derived chemicals, such as levulinic acid, furan dicarboxylic acid, furfuryl alcohol, tetrahydrofurfuryl alcohol, furan, tetrahydrofuran (THF), methyltetrahydrofuran (MTHF), dihydropyran, and acetylfuran.[6,12] China is the largest furfural producer in the world, with annual production exceeding 300 000 tons.[13] Recently, the conversion of xylan-type hemicellulose to a furfural platform has been widely reported, which can be performed by a one-step conversion process or two-step process with pretreatment and separation of the hydrolysate for subsequent upgrade.[14] Well-optimized procedures usually include the appropriate selection of catalysts, solvents, equipment, and process technology upgrades; these parameters have been considered for the integrated biorefineries and highly selective furfural production. A techno-economic analysis is crucial for evaluating the overall economic feasibility of industrial-scale furfural production.[15] An integrated biorefinery process for the co-production of furfural with other valuable chemicals can maximize the potential of lignocellulosic biomass residues, reduce waste and improve the overall economic viability. More stringent requirements have been proposed for modern furfural production processes based on the concept of green chemistry. Therefore, the objective of this article is to provide a systematic review of the catalytic transformation of lignocellulosic biomass, either as separate components or in entirety, into furfural using one-step and two-step strategies. In addition, techno-economic evaluations of the integrated biorefinery processes are provided and possible future outlooks and the scope for furfural production are discussed.

2. Hemicellulose resource

2.1. Xylan-type hemicellulose and its structure

Lignocellulosic biomass resources (LBR) can be divided into agricultural residues, forest residues, as well as herbaceous and woody energy crops.[16] The annual global production of LBR can reach 200 million tons.[17] The various types of hemicelluloses in LBR include xylans, xyloglucans (XGs) and β-glucans with mixed linkages and mannans, with xylans being the most abundant.[18] Xylan-type hemicellulose (xylans) can be divided into six structural subclasses: homoxylans (HOXs), (arabino)glucuronoxylans (AGXs), (glucurono)arabinoxylans (GAXs), glucuronoxylans (GXs), arabinoxylans (AXs), and heteroxylans (HTXs).[19] Mannans are hexose and the major constituent of hemicellulose in softwoods.[20] Xylans, which have higher C_5 sugar contents, are the optimal choice for XOS, xylose, and furfural production. *O*-Acetyl-4-*O*-methylglucuronoxylan (MGX) is the predominant component of hardwood hemicellulose (about 15–30%).[21] Most crop residues and grass seeds derived from food contain AGXs and AXs, respectively.[22] Unlike grass seeds, which are used as food ingredients, crop wastes, such as bagasse, corn straw, corncobs, rice straw, nut-shells, and oil crop waste, are the least utilized resources. For example, sugarcane bagasse, which is the main by-product of industrial sugar production, contains approximately about 26.5% hemicellulose and the hemicellulose content of corn

Table 1 Hemicellulose content and the main types of selected lignocellulosic substrates[38–60]

Classification	Lignocellulosic substrate	Hemicellulose (%)	Main type and structure	Ref.
Hardwood	Eucalyptus	11–13	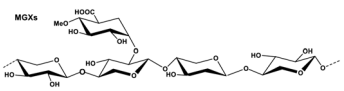	38 and 39
	Poplar	15–21		40
	Birch	20–23		41 and 42
Herbaceous plants and agricultural residues	Corncob	26–32.8	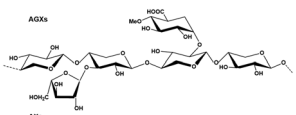	43 and 44
	Wheat straw	23.8		45
	Corn stover	19–22		46 and 47
	Switchgrass	20–31		48
	Camellia oleifera shell	27.94		49
	Sugarcane bagasse	26.5		50
	Rice straw	18.3		51
	Miscanthus	20–23		52
	Miscanthus × *giganteus*	22.3		53
	Peanuts	13.2		54
	Rice husk	18.3		55
	Barley husk	28.7		56
	Coconut husk	17.33		57
	Sweet sorghum bagasse	18–25.5		58 and 59
	Empty fruit bunches	25.3–33.8		60

cobs and corn stalks can be as high as 35%.[23] Seed shells, such as those of camellia, almonds, and walnuts, contain 25% xylan. These crop residues can provide an abundant amount of xylans for the selective preparation of functional oligosaccharides (XOS), furfural, and fermentable sugar substrates that can be used as sources of bioethanol.[24–26] The hemicellulose content, type, and structure of the various raw materials are summarized in Table 1.

2.2. Important furfural platform and formation mechanism

Furfural properties, derivatives and application. Regarding the physical properties, furfural can be directly used as an organic solvent to selectively extract aromatics and unsaturated compounds owing to its polarity and aromatic nature.[14] Chemically, two important groups (furan ring and aldehyde group) in furfural are highly reactive in various reactions, such as acetylation, acylation, reduction to alcohols, alkylation, hydrogenation, oxidation, decarboxylation, and amination reactions.[27] Furfuryl alcohol, 2-methylfuran, 2,5-dimethylfuran, and 2-methyl tetrahydrofuran can be obtained *via* the catalytic hydrogenation of furfural.[14] Maleic anhydrides, such as succinic, malic, and fumaric acids, can be obtained by selectively oxidizing furfural.[28] Furan, which is the simplest five-membered heterocyclic compound containing oxygen can be obtained by decarboxylation of furfural, which can be further hydrogenated to tetrahydrofuran.[29] Fuels and fuel additives, such as methylfurans, can be obtained *via* the etherification of furfural derivatives. Approximately 70% of the furfural produced is converted to furfuryl alcohol, solvents (tetrahydrofuran and 2-methyl tetrahydrofuran), fuel additives, and monomeric components for manufacturing polymeric materials and chemical intermediates for various synthetic applications.[30] Furan alcohol, the most important chemical derived from furfural, is primarily used in the production of resins in the foundry industry, and as a chemical building block for the synthesis of tetrahydrofurfuryl alcohol, ethyl furfuryl ether, levulinic acid, and γ-valerolactone (GVL).[28] Tetrahydrofuran is polymerized to polytetramethylene oxide and is also used as an industrial solvent for the production of polyvinyl chloride.[31] 2-Methylfuran and 2-methyltetrahydrofuran are good liquid fuel additives and solvents in organic and polymer chemistry, as well as chemical intermediates for drug synthesis.[32] The applications of furfural and its derivatives are listed in Table 2.

Furfural industry and market. Furfural was firstly isolated in 1821, and firstly industrialized by the Quaker Oats Company (Chicago, Illinois, USA) in 1921.[33] Later, other companies, for example, SupraYield® (South Africa, Australia), Westpro (China), Vedernikov (Russia), CIMV (France) and TU Delft (Netherlands) were also established based on the Quaker Oats technique.[34] These companies conventionally applied dilute sulphuric acid catalyzed percolation process for furfural production.[34] In the first step, the initial feedstock containing xylan, mainly sugarcane bagasse, crop straws or corncob, is hydrolyzed to produce pentoses, which are then cyclodehydrated to furfural in the second step. The furfural formed is recovered by steam distillation and fractionation.

Table 2 The applications of furfural and its derivatives[31,32,61]

Chemical name	Structure	Application
Furfural (FF)	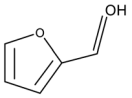	Solvent, lubricants, specialist adhesives, coatings, foams, weed killer, and flavour enhancer
Furfuryl alcohol (FA)	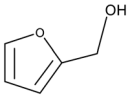	Resin, hypergolic starter fluids, surface coatings, mortar, resistant resins, boiler floor grouting, and adhesives
2-Methylfuran (2MF)	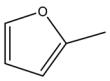	Pesticides, perfumes, pharmaceuticals, and fuel additives
Furan		Chemical intermediates
2-Methyltetrahydrofuran (2MTHF)	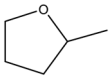	Gasoline additives, solvents, and chemical intermediates
Furoyl chloride	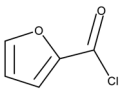	Drugs and insecticides
Tetrahydrofuran (THF)		Solvent, fuels, and fuel additives
Butane	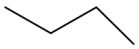	Transportation fuels
1,4-Butanediol	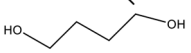	Plastic

Currently, the largest producer of furfural is located in China (~70% total production capacity).[35] Other countries, such as South Africa (20 000 t) and the Dominican Republic (32 000 t) contribute significant furfural production.[28] China and EU represent the largest and the second-largest markets with 55% and 15% of the global demand of furfural globally, respectively, which is expected to increase to 200 000 tons per year by 2030.[36] In 2004, furfural was listed as one of the 12 most promising platform chemicals by the U.S. Department of Energy.[37] Nowadays, the cost of furfural fluctuates between 800 and 1600 € per ton;[30] furthermore, its global market size was valued at USD 556.74 million in 2022, which is projected to increase to 700 $ million by 2024 at a compound annual growth rate of 4.9%.[27]

Mechanism for furfural formation. Furfural is the degradation product of hemicellulose, which undergoes hydrolysis to form pentose, followed by dehydration and cyclization to form furfural.

Glycoside bond hydrolysis of hemicellulose to form xylose. Brønsted acids (inorganic acids and organic acids with carboxylic and sulfonic functional groups) can be dissociated in water at high temperatures to release protons (H_3O^+); subsequently, the glycosidic linkage is initiated by protonation of either the glycosidic oxygen or ring oxygen to form a carbonium cation, which is followed by the C–O disruption of β-1,4-

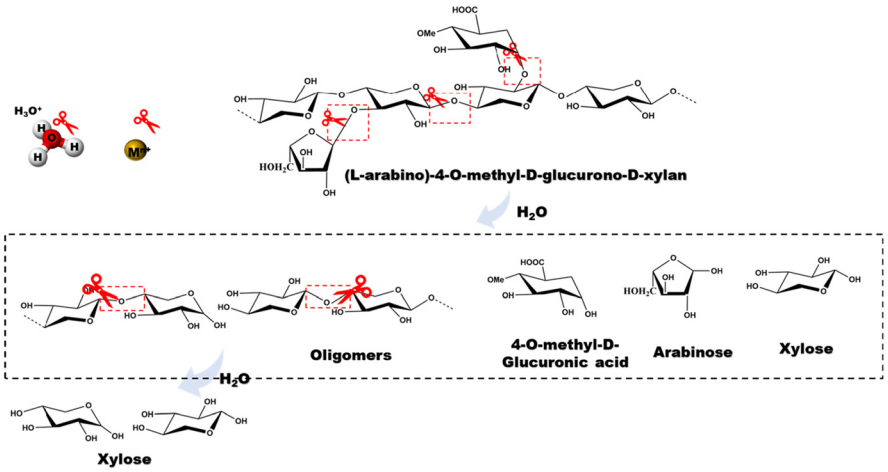

Fig. 2 Hydrolysis mechanism of xylan by acid catalysis.[62,63]

glycoside and hydrolysis of xylans to form XOS and xylose.[62] Lewis acids also can form H_3O^+ in high-temperature aqueous solutions. Water can be used as a Lewis base, and Lewis acids serve as electron pair acceptors that can react with a Lewis base to form a Lewis adduct, which can be expressed as $[M(H_2O)_x]^{n+}$ (where M is a metal element, x is the valence state, and n is a solvation number between four and nine).[63] In addition to H_3O^+, the metal cations also are responsible for the coordination of the glycosidic oxygen to facilitate the breakage of the glycosidic linkages (C–O–C).[64] Specifically, H_3O^+ from water autoionization at high temperatures is a co-catalyst in the additional acid hydrolysis process of hemicellulose, which synergistically accelerates the degradation of xylan into XOS and monosaccharides. Fig. 2 presents the hydrolysis mechanism of xylan-type hemicellulose by the catalysis of Brønsted acids and Lewis acids.

Xylose dehydration to form furfural. The formation of furfural from xylose with Brønsted acids catalysis involves two types of dehydration mechanisms:[65,66] acyclic and cyclic dehydration. Acyclic dehydration involves the formation of 1,2-enediol intermediates *via* enolization or a direct dehydration to produce 2,3-(α,β-) unsaturated aldehyde *via* β-elimination. In cyclic dehydration, the action of the H^+ on the O-2 of xypyranose results in the loss of one water molecule, forming 2,5-hydroxyfuranose *via* an intramolecular rearrangement, followed by two dehydration steps to produce furfural. Differently, Lewis acids catalyzed isomerization of xylose into xylulose *via* 1,2-hydrogen transfer, following further dehydration into furfural. The mechanism of the xylose dehydration process is shown in Fig. 3.

3. One-step and two-step approaches for furfural production

Because the production of furfural from lignocellulose hemicellulose first requires hemicellulose hydrolysis followed by the dehydration of pentosans, the strategy for furfural production can be divided into one-step and two-step approaches.

3.1. One-step approach for furfural production with homogeneous catalysts

The one-step approach involves the direct production of furfural from lignocellulose. The one-step approach for furfural production is listed in Table 3. A one-step conversion can also be conducted in a semi-batch process. Furfural can be obtained from biomass hemicellulose when a volatile stream (CO_2, water vapor, and acetic acid vapor) is used as a mobile phase in a semi-batch reactor. Continuous vapor is necessary to extract furfural into the stream from the feedstock as a fixed bed, and the vapor is then cooled to obtain liquid furfural. Mao *et al.*[67] proposed acetic acid as the volatile stream for the one-step extraction of furfural (Fig. 4a). The solid residue in the reactor was then processed *via* steam explosion to obtain a mixture of cellulose, soluble sugars, and lignin. Lignin can be obtained *via* alkali extraction and the soluble sugars can be obtained *via* direct water extraction. Specifically, the resulting furfural wastewater can be reused as an acetic acid source instead of a pure acetic acid stream for the next repetition, and recycled following the same procedure. The results demonstrated a higher furfural yield of 72.93% and selectivity of 73.49%; a comparable furfural yield can be obtained with reutilized acidic furfural wastewater.

A one-step conversion is more conducted in a batch process usually operated in a high-temperature and high-pressure autoclave. Mild initial temperatures and extremely acidic environment or higher initial temperatures and mild acidic environment are required for furfural production. In a concentrated acidic system, hemicellulose tends to first degrade into xylose, and the cellulose then begins to swell and dissolve when using concentrated hydrochloric acid (>20 wt%), sulfuric acid (>70 wt%), nitric acid (>42.24 wt%), or phosphoric acid (>80 wt%) as acid catalysts.[91] The separation of biomass hemicellulose and high furfural production can be achieved at mild

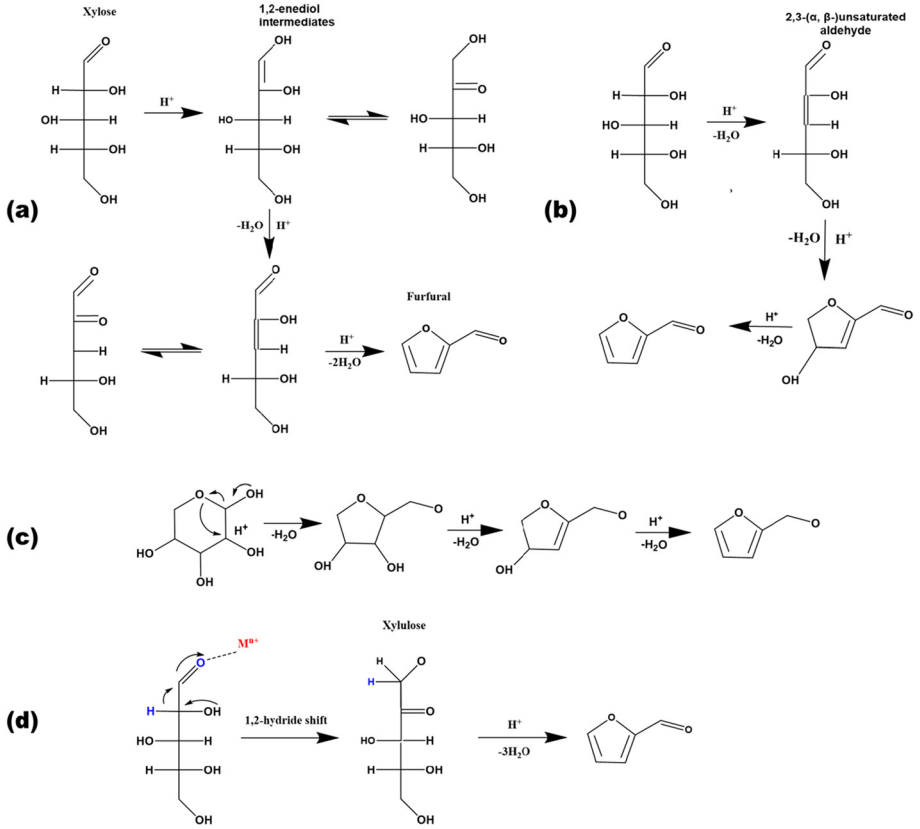

Fig. 3 Xylose dehydration for furfural formation *via* acyclic (a–b), cyclic dehydration (c) and 1,2-hydrogen transfer (d).[65,66]

temperatures (100–150 °C). The furfural yield of 50 mol% was obtained with concentrated formic acid (>64.40 wt%) at 150 °C.[92] However, concentrated acids are highly corrosive to equipment and are not sustainable. Dilute acid treatment is alternatively considered more accessible for commercialization than the aforementioned concentrated acid pretreatment owing to its lower corrosive effect on equipment, high catalytic effectiveness, low acid catalyst cost, and reduced acidic waste production.[93] Hemicellulose in dilute acid systems is mainly degraded into xylose, oligomers, and furfural according to a reported kinetic study.[94,95] Higher furfural yield can be achieved at higher treatment temperatures (>150 °C) with dilute acid catalysts. Ouyang *et al.*[68] investigated the use of dilute sulfuric acid for the one-step production of furfural from oil palm empty fruit bunches in a batch reactor (Fig. 4b). They developed a mechanism for the intermittent discharge of steam and proposed non-isothermal kinetics based on a considerable amount of xylan solubilized during the heating stage. The results demonstrated that the intermittent strategy resulted in a furfural yield of 71.4% at 160 °C for 5 h.

Homogeneous chloride-based salt solutions have been widely used for one-pot furfural production. Chen *et al.*[69] conducted a one-pot conversion of switchgrass to furfural, ethanol, and lignin using an aqueous choline chloride/methyl isobutyl ketone (ChCl/MIBK) biphasic solvent system. An acidic ChCl solution (0.6 wt% sulfuric acid) was used in the system for the pretreatment of switchgrass and further conversion of xylose; methyl isobutyl ketone (MIBK) was used as the organic upper layer for furfural extraction. Under optimized conditions (170 °C, 60 min, 10.7 wt% solid loading), a furfural yield of 84% was achieved; high-purity lignin and highly digestible pulp were simultaneously obtained. Jiang *et al.*[96] studied the role of ChCl as an additive in acidified water for furfural production starting from a highly concentrated xylose feed. The synthesis of choline xyloside was confirmed for the first time by HPLC-MS analysis. They proposed two possible reaction pathways: (1) 1-*O*-ChXyl protonation of choline xyloside, generation of oxocarbenium, and then formation of the tetrahydrofuran intermediate (Fig. 5a). (2) The generated choline xyloside intermediate undergoes ring contraction to form an oxonium ion while incorporating the choline fragment (Fig. 5b).

Metal halide salts have also been widely investigated as Lewis acid catalysts for one-step production of furfural. The selectivity of five metal salt catalysts ($AlCl_3$, $CuCl_2$, $CrCl_3$, $FeCl_3$, and $ZrOCl_2$) was evaluated for the one-step furfural production using tetrahydrofuran/water as the solvent phase.[72] The pH of the salts in high-temperature aqueous solution was in the order of $ZrOCl_2{\cdot}8H_2O$ < $FeCl_3{\cdot}6H_2O$ < $CuCl_2{\cdot}2H_2O$ < $AlCl_3{\cdot}6H_2O$ < $CrCl_3{\cdot}6H_2O$ when xylose was used as a substrate. $CrCl_3{\cdot}6H_2O$ catalysts achieved both the highest furfural selectivity and conversion rate. $FeCl_3$ reacted slower and required

Table 3 Acid catalysts used for the production of furfural from cellulosic biomass *via* a one-step process

Catalyst (organic solvent)	Raw material	Reactor	Pretreatment conditions (temperature–dosage–retention time)	Optimal furfural yield	Ref.
Acetic acid + $FeCl_3$ + HCl	Corncob	Semi-batch tubing-bomb reactor	190 °C–60 mM $FeCl_3$–30 min	72.93%	67
Sulfuric acid	Oil palm empty fruit bunch	Batch autoclave	160 °C–0.5%–5 h	71.4%	68
ChCl (MIBK)[a]	Switchgrass	Glass pressure tube	170 °C–70 wt% ChCl + 0.6 wt% H_2SO_4–60 min	84.04%	69
$CuCl_2$ [a]	Poppy stalks	Autoclave	200 °C–0.03 M–30 min	79.86%	70
$SnCl_4$	Corncob	Microwave reactor	190 °C–1%–0 min	9.0 wt% (based on the dry weight of corncob)	71
$FeCl_3$ (THF)[a]	Maple wood	Tube reactors	170 °C–0.1 M–30 min	95%	72
$AlCl_3$ + [BMIM]Cl[a]	Corncob	Microwave reactor	170 °C–0.25 mmol $AlCl_3$ + 2 g [BMIM]Cl–10 s	84.8%	73
LiBr·$3H_2O$ (dichloromethane)[a]	Corn stalk	Batch autoclave	120 °C–0.35 g LiBr·$3H_2O$ + 0.05 mol L^{-1} H_2SO_4–90 min	72.5%	74
H-ZSM-5 (γ-valerolactone)	Corn cob	Batch autoclave	190 °C–35 g L^{-1}–60 min	71.68%	75
H-ZSM-5	Flax straw	Batch reactor	250 °C–1 g–0 min	7.6%	76
Glu-TsOH-Zr (MTHF)	Fax straw	Batch autoclave	190 °C–0.5 g–120 min	About 22%	77
PA-FCB (GVL)	Corncob	Batch autoclave	195 °C–0.1 g –120 min	96.06%	78
$ZnCl_2$ + HCl + SO_4^{2-}/SnO_2-diatomite (GVL)	Corncob	Batch autoclave	170 °C–0.5 wt% HCl + 3.6 wt% SO_4^{2-}/SnO_2-diatomite + 15 g L^{-1} $ZnCl_2$–30 min	68.9%	79
SO_4^{2-}/CX-DMSn	Corncob	Batch autoclave	180 °C–0.32 g–5 h	65.74% (66.83% of selectivity)	80
ImmHSO_4-IL + NaCl (toluene)	Rice husk	Glass bottle	180 °C–25 mg ImmHSO_4-IL + 1.80 g NaCl–90 min	74.6%	81
$FeCl_3$ + NaCl (THF)	*Enteromorpha prolifera*	Batch autoclave	190 °C–12.5 Mm $FeCl_3$ + 2% NaCl–60 min	45.0 wt%	82
$SnCl_4$ + EMIMBr	Corn stalk	Glass vial	130 °C–23 mg $SnCl_4$ + 1000 mg EMIMBr–3 h	54.5%	83
HCl	Fax shives	Microwave reactor	180 °C–0.1 M HCl–20 min	72.2%.	84
H-SAPO-34 (GVL)[a]	Eucalyptus sawdust	Batch autoclave	210 °C–30 g L^{-1}–20 min	99.28%	85
p-Hydroxybenzenesulfonic acid-formaldehyde resin (GVL)	Corn stover	Batch autoclave	190 °C–0.2 g–100 min	50.3%	86
$Al_2(SO_4)_3$·$18H_2O$	*Cannabis sativa L. shives*	Bench scale reactor	160 °C–5%–90 min	62.7%	87
PW_{12}/ZSM-5 + LiBr	Aspen	Pressure tube	170 °C–25% LiBr + 10% PW_{12}/ZSM-5–6 h	29.9%	88
SO_4^{2-}/Sn-TRP-N (DMSO)	Corn stover	Batch autoclave	190 °C–10 wt%–3 h	77.82%	89
$AlCl_3$ + NaCl (MTHF)	Sugar cane bagasse	Microwave reactor	190 °C–0.1 M $AlCl_3$ + 10 wt% NaCl–45 min	58.6%	90

[a] Indicates the furfural yield can reach 70% in moderate conditions (120–170 °C, ≤90 min or 180–210 °C ≤30 min) with alternative inorganic acid catalysts.

20 min to reach a similar furfural selectivity of 65%. Notably, when the reaction substance was changed to maple wood, $CrCl_3$ did not produce high furfural yields despite having high Lewis acidity, which caused xylose to rapidly dehydrate and degrade. $FeCl_3$ demonstrated the best performance and achieved the highest furfural yield of 95%, outperforming sulfuric acid and the other four metal halides. Hoşgün *et al.*[70] found that $CuCl_2$ demonstrated an extreme performance and presented a maximum efficiency for furfural production (79.86%) from poppy stalks under one-pot hydrothermal reaction conditions at 180 °C. Wang *et al.*[97] found that $SnCl_4$, which had the lowest pH, achieved a superior furfural yield from beech xylan compared to other high-valence chloride salts ($InCl_3$, $GeCl_4$, $AlCl_3$ and $FeCl_3$). Furthermore, the 2-MTHF/water (2/5, v/v) system improved the furfural yield and selectivity. The optimal furfural yield was 78.1% in a 2-MTHF/H_2O biphasic system using $SnCl_4$ as an effective catalyst. The ratio of organic solvent/H_2O is an important variable. The other optimal ratios of GVL/H_2O (25%, v/v) and H_2O/DMSO (5/5, v/v) were also confirmed to be desirable for promoting the formation of furfural and suppressing side reactions.[98,99] However, a study indicated that the efficient synthesis of $SnCl_4$ and $MgCl_2$ as catalysts in a single ionic liquid, 1-ethyl-3-methylimidazolium bromide (EMIMBr), for the one-pot conversion of corn stalk to furfural was more effective than that in organic solvent/EMIMBr biphasic systems, with furfural yields as high as 54.5%.[83] In a study conducted by Zhang *et al.*, the paired $CrCl_3$/$AlCl_3$ catalyst demonstrated a higher furfural

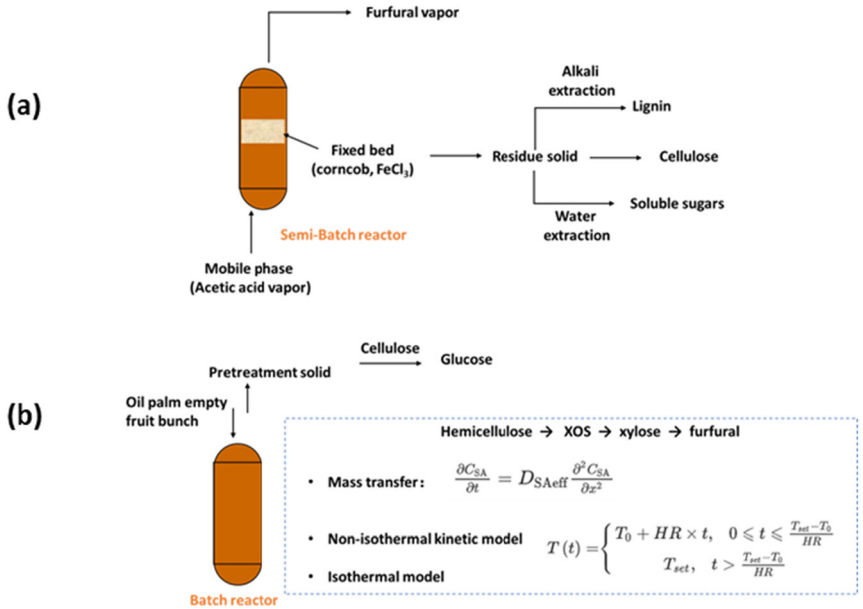

Fig. 4 One-step furfural production from biomass in a semi-batch (a) and batch reactor (b).

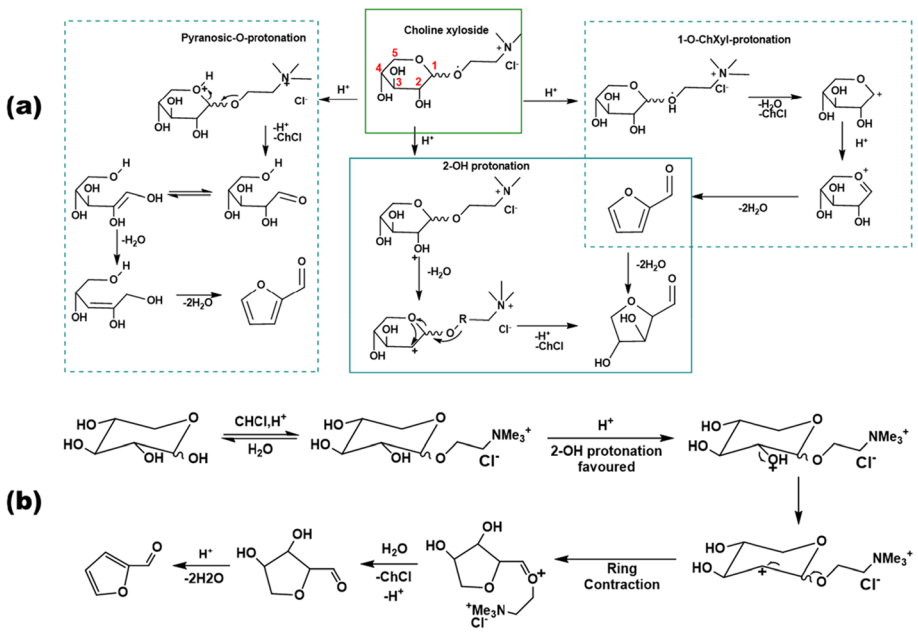

Fig. 5 Mechanisms of xylose dehydration with ChCl as catalyst: 1-*O*-ChXyl protonation of choline xyloside (a), ring contraction of choline xyloside to form an oxonium ion (b).[96]

yield from corncobs than that of other paired salts and $CrCl_3$ alone in the following order:[73] $CrCl_3/AlCl_3$ > $FeCl_3{\cdot}6H_2O/AlCl_3$ > $CuCl_2{\cdot}2H_2O/AlCl_3$ > $SnCl_2{\cdot}2H_2O/AlCl_3$ > $CeCl_3{\cdot}7H_2O/AlCl_3$ > $CrCl_3$. In addition, Lyu *et al.*[100] proposed three tools (Lewis acid strength, oxidizing properties, and solubility products of the corresponding hydroxides) to quickly screen ideal catalysts for furfural production and to investigate the factors that inhibit furfural production. Metal ions with higher Lewis acid strengths are more favorable for furfural production. A higher standard reduction electrode potential (SREP) of an ion (more positive) indicates its stronger oxidizing property. High solubility products of metal hydroxides can decrease the consumption of catalysts during hydrolysis. The degradation of furfural can be observed based on the formation of humins and oxidation of the reaction substrate (CO_2 and CO gas composition change). Therefore, they concluded that the ideal catalyst for furfural production should have a strong Lewis acid strength, weak oxidizing property, and high solubility product of the

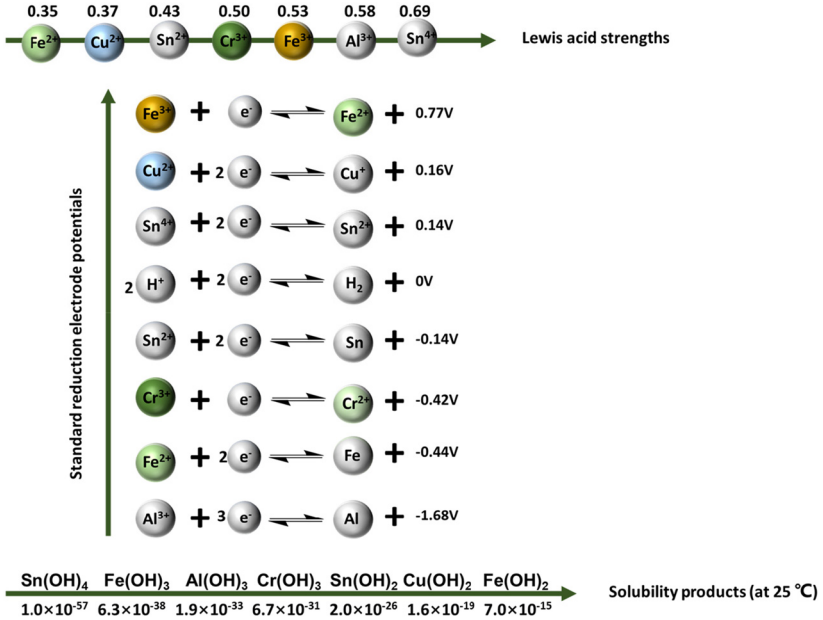

Fig. 6 The order of the Lewis acid strengths of several metal ions, standard reduction electrode potentials and solubility of the corresponding hydroxides.[100]

corresponding hydroxide; the factors that inhibit furfural production are humins and the oxidation reaction of corncobs and xylose. The order of the Lewis acid strengths of several metal ions, the standard reduction electrode potentials, and solubilities of the corresponding hydroxides are shown in Fig. 6.

Molten metal-salt systems can achieve higher furfural yields under mild conditions. Li *et al.*[74] evaluated the conversion of corn stalk to glucose and furfural in a molten salt hydrate/organic solvent biphasic system ($LiBr{\cdot}3H_2O$/dichloromethane). Under the optimal reaction conditions (0.05 mol L^{-1} H_2SO_4, 120 °C, 90 min), 58.9% glucose and 72.5% furfural were yielded by the one-step process. $LiCl{\cdot}3H_2O$ acted both as the solvent and catalyst for the synthesis of furfural from xylan, reported by Liu *et al.*[101] A close furfural yield of 41.63% was achieved in a more severe condition (140 °C for 2 h) compared to that of the aforementioned study by Li *et al.* The GVL solvent was found to be more effective than other polar aprotic solvents (MIBK, THF, DMSO, sulfolane) used to enhance the furfural yield; an increasing yield (56.68%) was observed in the biphasic system. A maximum furfural yield of 77.22% was achieved with a 1 : 2 mass ratio of GVL to $LiCl{\cdot}3H_2O$ combined with 0.15 mmol of $Al_2(SO_4)_3$ as the co-catalyst. The reaction pathway for the conversion of xylan to furfural in the GVL/$LiCl{\cdot}3H_2O$ biphasic system was revealed. Xylan is initially depolymerized into xylose under the catalysis of Brønsted acid followed by isomerization, cyclization, and dehydration (Fig. 7a). The catalysts were first hydrolyzed to form the intermediates $[Li(H_2O)_6]^+$ and $[Al(OH)_{2(aq)}]^+$, and $[Al(OH)_{2(aq)}]^+$ and Cl^- then promoted the transfer of 1,2-hydrogen between C1 and C2 (Fig. 7b).

The introduction of metal salts into DES systems can promote the production of furfural. An $AlCl_3$-catalyzed ChCl-oxalic acid/MIBK biphasic system was developed for furfural production from eucalyptus, which obtained a yield of 70.3% under the optimal pretreatment conditions (at 140 °C for 90 min).[102] The performance of $FeCl_3$, $AlCl_3$, $SnCl_4$, and $TeCl_4$ in an aqueous choline chloride-oxalic acid (16.4 wt% H_2O) DES system was investigated for producing furfural from oil palm fronds (OPFs).[103] In this co-catalyst system, Brønsted acid supplied by oxalic acid from DES is responsible for breaking the β-1,4 glycosidic bonds of hemicellulose to form xylose *via* hydrolysis; subsequently, the Lewis acids catalyze the isomerization of xylose to xylulose *via* an intramolecular 1,2-hydride shift pathway similar to that in the previous study. The χ/r^2 values, denoting the electric field gradient around the cation, of four metal chlorides were found to obey the following trend: $Te^{4+} > Sn^{4+} > Al^{3+} > Fe^{3+}$. The results demonstrated that although ADES-$TeCl_4$-OPFsOPFs achieved a relatively lower furfural yield of 55.6% than ADES-$AlCl_3$-OPFs (60.2%) and ADES-$SnCl_4$-OPFs (59.4%), the lower amounts of $TeCl_4$ (2.5%) and $SnCl_4$ (0.25%) were required for a similar furfural yield. Therefore, they concluded that $TeCl_4$ with a higher χ/r^2 value demonstrated to be the stronger Lewis acid, thus more quickly catalyzed the degradation reaction of furfural. Furthermore, the addition of Lewis acids also enhanced the acidity of the Brønsted acid *via* synergistic DES–Lewis acid catalyst interactions. Fig. 8 presents the proposed mechanism of the $SnCl_4$ and ChCl-oxalic acid interactions for furfural production.

Acidic ILs can be used as catalysts and (or) solvents for the one-step production of furfural. Peleteiro *et al.*[104] reported the production of furfural from eucalyptus wood using a Brønsted acid ionic liquid (1-butyl-3-methylimidazolium hydrogen sulfate) as both a solvent and a catalyst in the presence of a co-

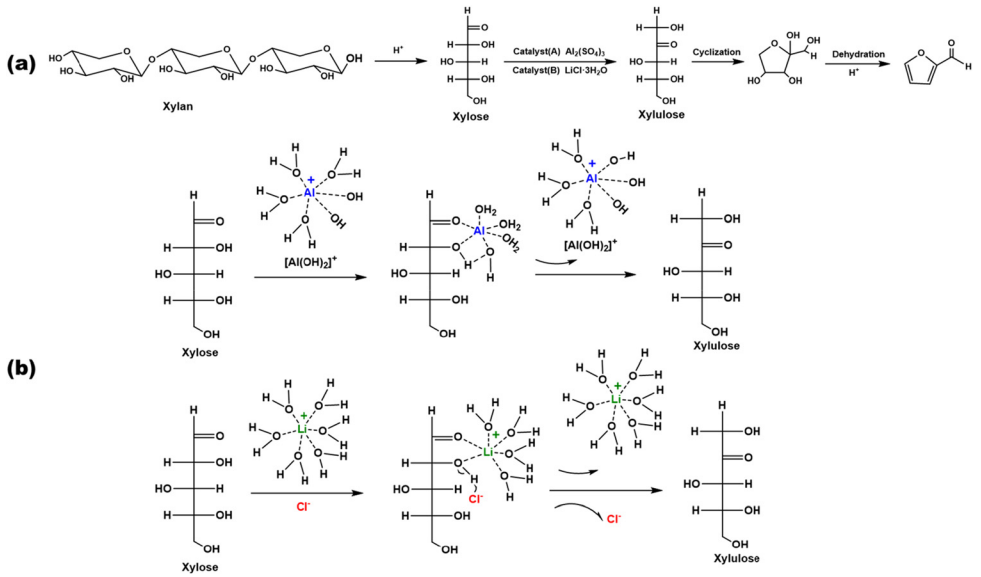

Fig. 7 The dehydration mechanism of xylose with $Al_2(SO_4)_2$ (a) and $LiCl_3$ (b) as Lewis acid catalysts.[101]

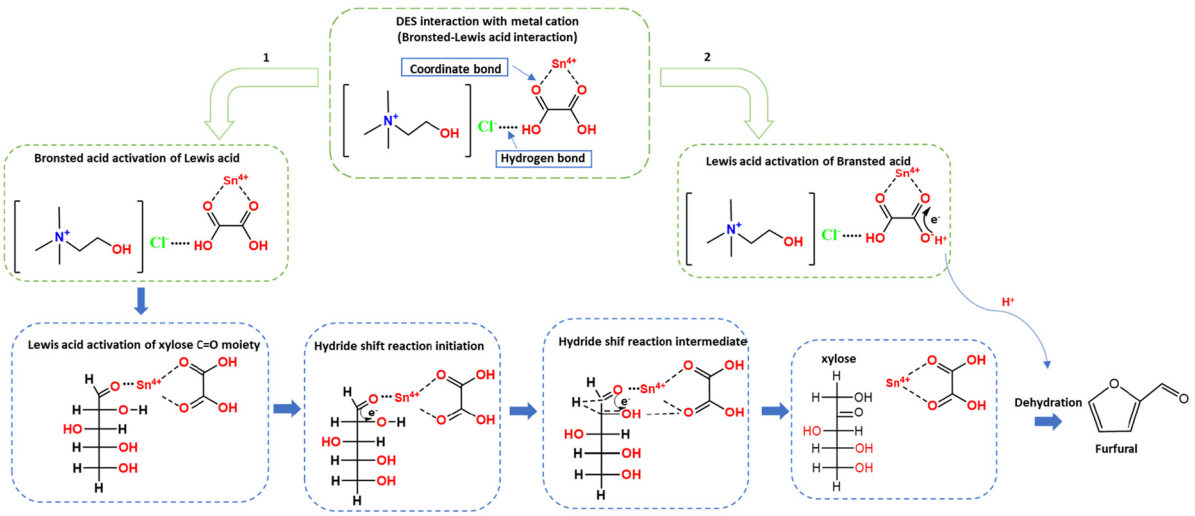

Fig. 8 The proposed mechanism of $SnCl_4$ and ChCl-oxalic acid interactions for furfural production.[103]

solvent (dioxane). An optimal furfural conversion (59.1%) was achieved at 160 °C. In addition, the reported $ImmHSO_4$-IL catalyst exhibited a higher catalytic activity than those prepared using other immobilized imidazolium acid ionic liquid catalysts ($ImmCH_3SO_3$-IL and $ImmH_2PO_4$-IL), and achieved the highest furfural yield of 74.6% from rice husk.[81]

3.2. One-step approach for furfural production with heterogeneous catalysts

In addition to homogeneous acids, heterogeneous catalysts for the one-pot conversion of lignocellulose biomass have gained increasing attention owing to their simple separation after the reaction and reutilization.[79] Heterogeneous catalysts can be divided into Lewis acid catalysts alone, Brønsted acid catalysts alone and the combination catalysts of two acid sites. H-ZSM-5 is an acid catalyst with only Lewis acid site. Harry *et al.*[76] indicated that H-ZSM-5 is a high-performance zeolite catalyst with a high silica-to-alumina ratio for a high yield of furfural from flax straw in a batch reactor. Shorter reaction times minimize the formation of undesired liquid by-products, enhancing the selectivity and yield of furfural in subcritical water. The H-ZSM-5 catalyst was more favorable for the formation of furfural when HCl was not used as a co-catalyst. A furfural yield of 7.6% (based on the mass of flax straw) was achieved at an optimal condition (250 °C, 6.0 MPa, flax straw mass fraction of 5%, and 0 retention time, 1 g H-ZSM-5).

Carbon-based solid acids bearing multiple Brønsted acid sites (inherent –OH, –COOH, and additional $–SO_3H$ groups

after sulfonation) were also investigated, which exhibited excellent performances ascribed to the synergic effect of these groups in the catalytic production of furan derivatives.[105] A phosphotungstic acid-functionalized biochar (PA-FCB) in the γ-valerolactone/subcritical water solvent demonstrated a high furfural yield of 96.06% at 468 K for 120 min.[78] Satisfied furfural yields of 95% and 77.4% were obtained from corn cob and rice husk, respectively, by the one-pot transformation process with nitrogen doped carbon solid acids in γ-valerolactone as a catalyst at 170 °C for 45 min.[106]

Some solid acids with both Brønsted and Lewis acid sites were also reported. A sulfonated carbon-based zirconia (Glu-TsOH-Zr) demonstrated good catalytic activity, resulting in a 40% increase in the furfural yield from fax straw biomass at 190 °C after 120 min in a stainless-steel batch reactor; a recyclability investigation of the catalyst revealed only a 5% loss.[107] A unique carbonized core–shell diatomite (SO_4^{2-}/CX-DMSn) with Lewis and Brønsted acid sites was prepared and exhibited an excellent catalytic ability.[80] The results demonstrated a furfural yield of 65.74% and a selectivity of 66.83% for corncob. Compared with SO_4^{2-}/SnO_2-diatomite, additional liquid Brønsted acid catalysts can enhance furfural production. HCl is inexpensive and has been found to be more effective than H_3PO_4, HNO_3, and H_2SO_4 in the hydrolysis of lignocellulose biomass.[108] The dilute HCl-assisted solid acid (SO_4^{2-}/SnO_2-diatomite) one-pot catalysis of corncob to furfural in γ-GVL–water media was investigated, confirming that Brønsted acids with lower acid dissociation constant (pK_a) values (stronger hydrogen donor capacity) had higher turnover frequency (TOF) values as follows: HCl ($pK_a = -7.0$) > H_2SO_4 ($pK_a = -3$) > oxalic acid ($pK_a = 1.25$) > fumaric acid ($pK_a = 3.15$) > citric acid ($pK_a = 3.14$) > D,L-malic acid ($pK_a = 3.49$) > formic acid ($pK_a = 3.75$) > succinic acid ($pK_a = 4.16$) > acetic acid ($pK_a = 4.75$).[79] Furthermore, γ-GVL–water as a biphasic system exhibited a better furfural yield compared to other organic solvents (toluene, glycerol, glycol, isoamylol, dibutyl phthalate, butyl acetate, *n*-butanol). An appropriate volumetric ratio of γ-GVL increased the furfural yield. A high furfural yield (68.9%) was achieved from corncob under the optimal conditions (170 °C, 30 min, 0.5 wt% HCl, 3.6 wt% SO_4^{2-}/SnO_2-diatomite, ratio of γ-GVL : water was 6 : 4, v/v).

Solid acid catalysts own the characteristics of good thermal stability, high reusability and chemical stability. The prepared SO_4^{2-}/SiO_2-Al_2O_3/La^{3+} only observed a decline of 5.28% yield of furfural after four runs.[109] A dual-functional carbon-based solid acid catalyst (DFCSA) with tunable Brønsted acid sites (H_3PO_4 and HNO_3) and Lewis acid site ($Al(NO_3)_3$) displayed excellent hydrothermal stability, with only a slight degradation in activity after 10 cycles.[110] A commercially available sulfonic acid-containing heterogeneous Brønsted acids (Amberlyst 45) was found to show higher hydrothermal stability at hydrothermal flow conditions of 160 °C, with <10% loss in acidity after 48 h.[111] Although a good performance of catalysts has been achieved, the deactivation and regeneration of heterogeneous catalysts still face some challenges. In fact, the activity loss of Brønsted acid-functionalized carbon-based solid acid catalysts was mainly due to the reduced number of Brønsted acid sites responsible for the recycle performance. Sulfonic-acid groups in a sulfonated activated carbon are prone to leaching in hydrothermal reaction environments because of the tendency of the C–S bond to undergo desulfonation.[112] The degree of desulfonation (sulfonic acid group density) decreased from initially 0.58 mmol g^{-1} to 0.35, 0.30, and 0.20 mmol g^{-1} after treatment at 150, 200, and 225 °C in hot compressed water,[113] which indicates that desulfonation increases with increasing reaction severity. Besides sulfonic acid group leaching, a hitherto unknown mode of deactivation was identified that proceeds by ion-exchange processes with cationic mineral species.[112] In addition to the leaching of sulfonic acid residues, the deposition of carbonaceous residues in the hydrothermal process also result in catalyst deactivation.[114] Use of a polar aprotic solvent is a successful approach to minimize fouling.[111] Carbonaceous residues removal for regeneration of catalysts can be achieved *via* oxidation, gasification or hydrogenation.[114] In conclusion, the degradation of catalysts is unavoidable due to the decrease of acid density and the increase of fouling deposition. Biocarbon-based solid acids can be prepared again by re-carbonization and sulfonation due to their low cost and ease of preparation. Commercially expensive or complex solid acids hard to prepare, such as zeolites or resins, can regenerate by coke removal to extend their life span after carbon plugging.

3.3. Two-step approach for furfural production with the same catalysts

The two-step process requires an additional separation of the hydrolysate. In the first step, the raw materials are pretreated at a mild temperature to obtain pentosan-rich hydrolysates, and cellulose is mostly retained in the solid fraction. After the separation *via* solid–liquid filtration, in the second step, the filtrate liquids mainly containing xylose and xylo-oligosaccharides were subjected to further reactions to generate furfural under more severe conditions. The two-step approach enables using pretreated feedstock for further utilization. The two-step process for furfural production is listed as Table 4.

A high-pressure CO_2 and H_2O-assisted process was reported for the two-step selective conversion biomass hemicellulose into furfural.[117] Subcritical water as a solvent at a temperature above its boiling point but below the critical point at a certain pressure can generate hydronium ions, which act as effective catalysts for the breakdown of hemicellulose.[125] Carbonic acid formed by CO_2 dissolved in water can effectively promote the hydrolysis of hemicellulose in biomass and the production of hemicellulose-derived sugars compared to the CO_2-free autohydrolysis process.[126,127] Hemicellulose solubilized in the liquid phase can be subjected to subsequently convert into furfural or carboxylic acids. The hemicellulose hydrolysate dehydration yielded 43 mol% of furfural with a selectivity of 44 mol% in a biphasic system with water/THF/MIBK under optimal conditions (initial CO_2 pressure of 50 bar, 180 °C, 60 min). Additional dilute acids can also promote hydrothermal autocatalytic processes and reduce the reaction temperature. Cornejo

Table 4 Acid catalysts used for the production of furfural from cellulosic biomass *via* a two-step process

Catalyst (organic solvent)	Raw material	Reactors	Pretreatment conditions (temperature–dosage–retention time)	Optimal furfural yield	Ref.
ChCl/*P*-toluenesulfonic acid[a]	Corncob	Glass bottle	160 °C–1.8%–80 min	70%	9
NaCl (GVL, THF)	*Pubescens*	Batch autoclave	200 °C–5%–2 h	76.9 mol% with 82.2% selectivity	98
$AlCl_3$ + ChCl-oxalic acid (MIBK)[a]	Eucalyptus	Batch autoclave	140 °C–25.0 g DES + 95.6 mg $AlCl_3{\cdot}6H_20$–90 min	70.3%	102
Chloride-oxalic acid DES + $SnCl_4$	Oil palm fronds after ultrasonic irradiation	Glass beaker	120 °C–88.0 mmol DES + 2.50 wt% $SnCl_4$–45 min	59.4%	103
[bmim]HSO_4 (dioxane)	Eucalyptus	Batch autoclave	160 °C–10 kg (based on 1 kg wood)–4 h	59.1%	104
Supercritical CO_2 + H_2SO_4	Rice husk	Semi-batch reactor	180 °C–1836 g CO_2 + 7% H_2SO_4–3 h	90%	115
Methanesulfonic acid	Bagasse	Glass ampoules	180 °C–0.1 M–20 min	About 85 mol%	116
High-pressure CO_2 (THF/MIBK)	Wheat straw	High-pressure Parr 4655 reactor	180 °C–60 min	43 mol% with a selectivity of 44 mol%	117
ChCl-oxalic acid	Oil palm fronds	Schott bottle	100 °C–1.234 g L^{-1}–135 min	26.34%	118
Maleic acid	Corn stover	Microwave reactor	200 °C–0.25 M–28 min	61%	119
$SO_4^{2-}/SiO_2{-}Al_2O_3/La^{3+}$	Corncob	Batch reactor	150 °C–0.01 g–150 min	21%	120
ChCl-H_2SO_4	Switchgrass	Pressure tube	150 °C–2% $AlCl_3$–15 min	60%	121
$MgCl_2$ + ChCl/HCl (2-Me-THF)[a]	Corn stover	Batch autoclave	120 °C–15 g L^{-1} $MnCl_2$ + 5 mL DES–60 min	86.94%	122
[C4mim]HSO_4 and [C_3SO_3Hmim]HSO_4[a]	*Eucalyptus nitens* wood	Microwave reactor	180 °C–1.16 mol L^{-1} [C4mim]HSO_4–30 min 180 °C–0.049 mol L^{-1} [C_3SO_3Hmim]HSO_4–5 min	75.0 ± 0.71% with [C4mim]HSO_4 as a catalyst and (85.6 ± 0.32%) [C_3SO_3Hmim]HSO_4 as a catalyst	123
H_2SO_4	Corn stover	Batch autoclave	210 °C–5 mL–20 min	46.5%	124

[a] Indicates the furfural yield can reach 70% under mild conditions (120–170 °C, ≤90 min or 180–210 °C, ≤30 min) with alternative inorganic acid catalysts.

et al.[128] reported a two-step biorefinery process for the production of glucose and furfural from wheat straw and poplar chips. Thermochemical pretreatment with dilute H_2SO_4 as the catalyst was conducted for hemicellulose hydrolysis in the first step, which was followed by microwave-assisted cyclodehydration of xylose in a MIBK solvent in the second step for furfural production. Up to 12.6 kg of glucose and materials and 2.5 kg of furfural can be produced starting from 50 kg of biomass. Maleic acid has been reported to be an organic acid catalyst for selectively depolymerizing plant hemicellulose to xylose and dehydrating the resulting xylose to furfural in a microwave-assisted two-step process.[119] Similar furfural yields were obtained from xylose hydrolysates of corn stover (61%) and pure xylose (67%), but in nearly half the time of the latter (Fig. 9a). $SO_4^{2-}/SiO_2{-}Al_2O_3/La^{3+}$, as a solid acid catalyst, was applied for the two-step furfural production from corncobs, obtaining a maximum furfural yield of up to 21% at 190 °C for 60 min in the hydrothermal process.[120] A multistep recycling method for enriching hemicellulose-derived sugars was also proposed. Chen *et al.*[121] reported aqueous choline chloride as a novel solvent for the two-step furfural production from switchgrass fractionation. Under a relatively mild pretreatment condition (120 °C, 25 min), acidified ChCl solution (pH = 1.11) efficiently removed 76% of xylan. After five cycles, xylose-enriched liquor was used as the reaction substrate for furfural production, resulting in a yield of 48.22%, and 93% lignin removal from switchgrass.

ChCl-based DESs are reportedly easy to prepare and are inexpensive green liquids that are effective for lignocellulose biomass pretreatment.[129] A three-constituent DES (choline chloride-oxalic acid-ethylene glycol) removed 91.09% of xylan from bamboo-based hemicellulose and the introduction of ethylene glycol into the DES can decrease the condensation of lignin.[130] The pH of DES is considered an important variable for enhancing catalytic activity. *p*-Toluenesulfonic acid (*p*-TsOH) is a strong organic acid. ChCl/*p*-TsOH (1 : 1 molar ratio) DES was used as the solvent and catalyst for the two-step furfural production, obtaining a final optimal furfural yield of 69.8%; 97.5% of the furfural can be recycled by 1-tetradecanol and thymol based on the hydrophobic deep eutectic solvents.[9] The ChCl/*p*-TsOH DES was found to be the best with a lower pH value of 1.0 compared to the other ChCl/oxalic acid and ChCl/levulinic acid DESs with the same 1 : 1 molar ratio, and achieved a furfural yield of 85% in 1.5 h at 120 °C (ref. 131). The integrated biorefining of deep eutectic solvents (ChCl/*p*-TsOH) for furfural production was studied.[9] First, hydrolysis of the corncob xylan was performed at 140 °C for 20 min, followed by recycling the corncob hydrolysate for 3 runs to obtain a concentrated liquor (11.6%). Subsequently the dehydration of the xylose-rich corncob hydrolysate at 200 °C and 120 min of nitrogen stripping was performed in the second step, using hydrophobic deep eutectic extraction solvents (Tdec : Thy) as an alternative to energy intensive distillation operations for the

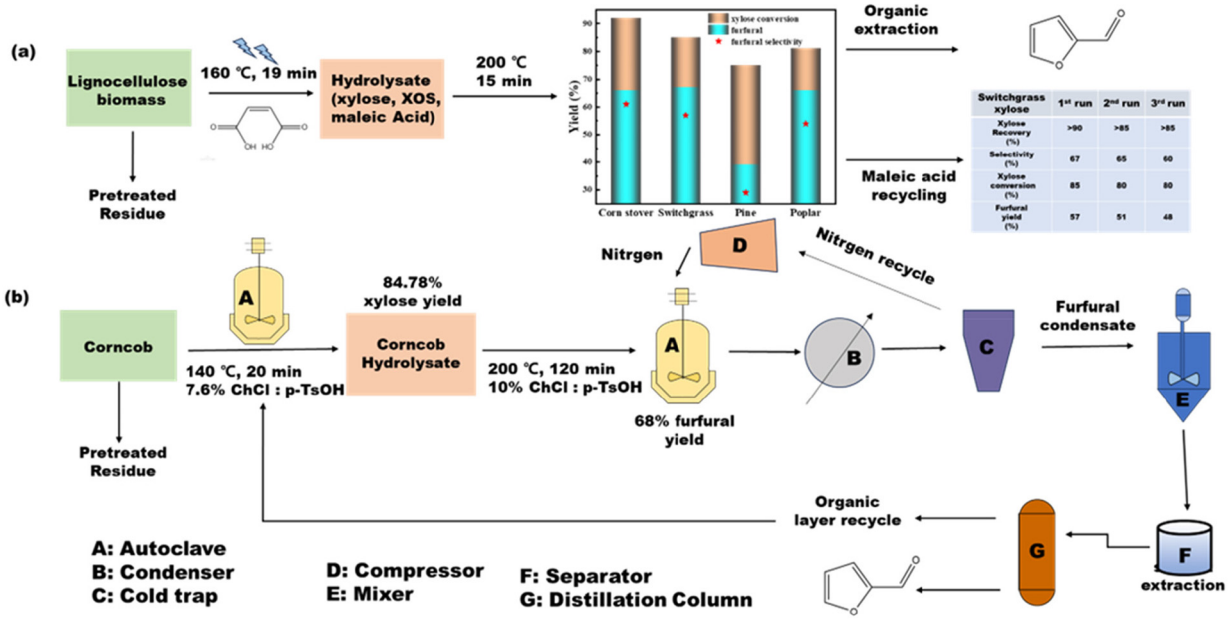

Fig. 9 Two-step process for furfural production *via* maleic acid (a) and ChCl : *p*-TsOH (b).[119,121]

isolation and purification of furfural from the aqueous condensate obtained, finally resulting in an optimal furfural yield of 69.85% from corncob (Fig. 9b). Hu *et al.*[122] developed an integrated strategy for the two-step hemicellulose-to-furfural conversion from corn straw in an aqueous DES (ChCl/hydrochloric acid)/2-Me-THF solvent. The aqueous DES resulted in a furfural yield of 86.94% from hydrolysate obtained after the dilute-acid pre-hydrolysis of lignocellulose, and a DES recycled yield of 85% was achieved. The lignin and cellulose were then separated from the solid residue using the same aqueous DES. They proposed that Cl^- ions present in ChCl can facilitate 1,2-hydrogen transfer reactions, resulting in the formation of isomeric xylulose, which exhibits a higher reactivity compared to xylose and is more prone to dehydration and cyclization to form furfural under acidic conditions (Fig. 10).

3.4. Two-step approach for furfural production with different catalysts

Both hemicellulose and lignin can be separated when the reaction is performed in an organic solvent, a DES or an IL, leaving a cellulose-rich solid residue. Lignin can regenerate *in situ* after the addition of a certain amount of water. Thus, hemicellulose-derived sugar hydrolysates can be selectively obtained for upgrade *via* a two-step process using additional catalysts. GVL is a green solvent with an excellent delignification ability. Luo *et al.*[132] converted pubescent hemicellulose to furfural in a GVL/water co-solvent in an autoclave using a simple two-step process (Fig. 11a). First, the co-dissolution of hemicellulose (93.6 wt%) and lignin derivatives (80.2 wt%) was promoted *via* hydrothermal autocatalysis at 160 °C, leaving a high purity cellulose. Second, furfural was prepared by adding NaCl and THF at a higher temperature (200 °C), resulting in a yield of 76.9 mol% and selectivity of 82.2%. Moreover, the interaction mechanism of NaCl with the hemicellulose-derived oligomers and monomers was revealed. The results demonstrated that Cl^- is a good hydrogen acceptor, and can form hydrogen bonds with C-OH-2,3,4 in xylose with the help of H_2O. The dehydration of xylose to form furfural *via* the intermediate xylulose in an isomerization reaction, first occurred on the C-OH-4 of xylose and then on the C-OH-2,3 of xylose (Fig. 11b).

Acidic ionic liquids have been proposed as environmental friendly catalysts for the two-step furfural production. Penín *et al.*[123] combined hydrothermal processing with an acidic ionic liquid, 1-butyl-3-methylimidazolium hydrogen sulfate

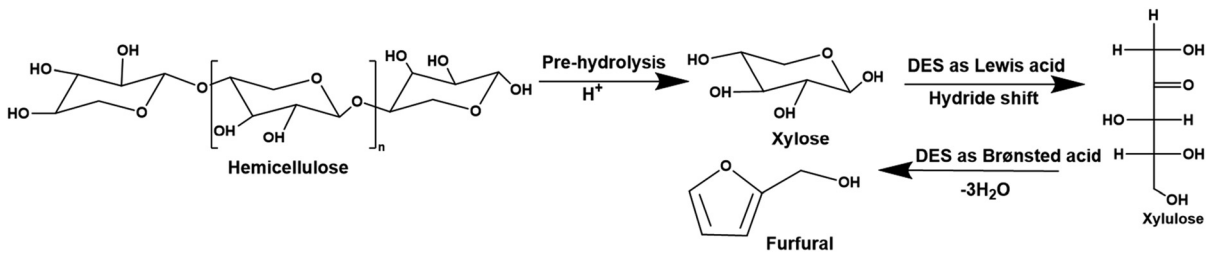

Fig. 10 The proposed mechanism of DES for furfural production.[122]

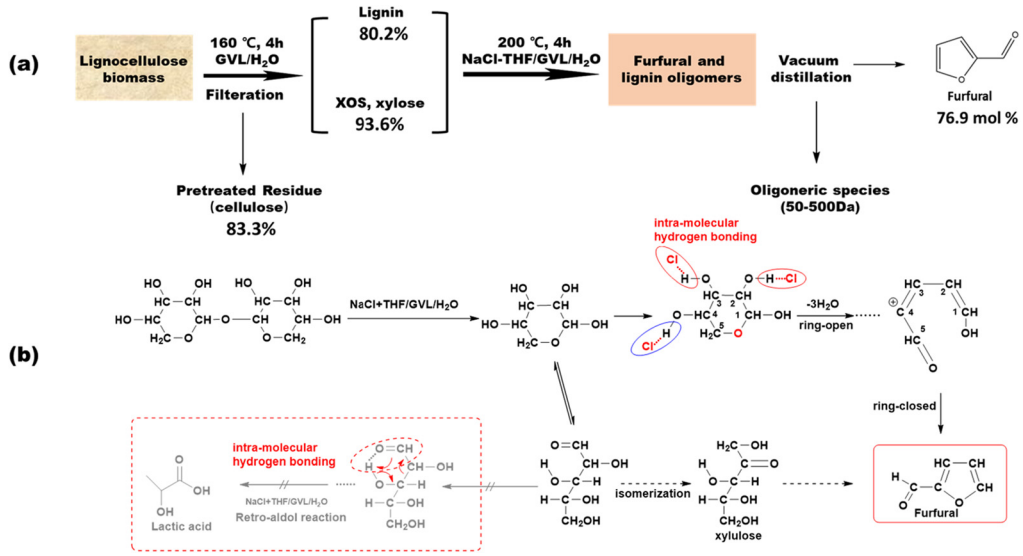

Fig. 11 The two-step process (a) and proposed mechanism of NaCl+THF/GVL/H_2O system (b) for furfural production.[132]

([C4mim]HSO_4), and 1-(3-sulfopropyl)-3-methylimidazolium hydrogen sulfate ([C3SO_3Hmim]), as substrates in the second step in a water/methyl isobutyl ketone biphasic medium for furfural production. Under the selected operational conditions, the molar conversions of the precursors (pentosans) into furfural were 75.0 ± 0.71% with 1.16 mol [C4mim]HSO_4/L as the catalyst, and 82.5 ± 0.91% with 0.049 mol [C3SO_3Hmim]HSO_4/L as the catalyst at 180 °C. Another acidic ionic liquid, 1-butyl-3-methylimidazolium hydrogen sulfate ([bmim]HSO4), was used as a catalyst for furfural production from wood-derived liquid streams after hydrothermal treatment in water/MIBK media.[133] The results indicated that maximum furfural production was (61.6%) achieved under the optimal operational conditions (140 °C, 6 h reaction time, and catalyst loading = 0.3 g g^{-1} water). The recovery and cycling of ILs are necessary for cost-saving, owing to the high purchase cost. A satisfactory catalytic activity with [bmim]HSO_4 as a catalyst was also observed despite undergoing eight consecutive runs (conversion range, 60.1–66.7%).

3.5. Summary

In summary, the two-step process for furfural production based on the obtained prehydrolysate has a low initial input energy, but requires an additional separation unit. To achieve a one-step production of furfural from biomass, higher-intensity treatment conditions are required to degrade the resistant structure of the cell wall and dehydrate xylose. A one-step process requires continuous vapor or water steam to extract furfural when the reaction is operated in a semi-batch reactor, and an acidic system is necessary for hemicellulose hydrolysis and xylose dehydration. Catalysts and solvents are crucial for increasing reaction rates. Cl^- anions are reportedly more efficient for enhancing the formation of isomeric xylulose from xylose. Halide salts with higher pK_a values and valences tend to exhibit stronger catalytic activity with lower pH values of a solution. Trivalent metal salts, such as $FeCl_3$ and $AlCl_3$, are better candidates for furfural production from lignocellulosic biomass. Paired cocatalysts can further improve the furfural yield. A synergistic DES–Lewis acid catalyst interaction increases the acidity of the solution. An appropriate ratio of solvent/H_2O (usually 10–50%, v/v) can improve the selectivity of furfural. A decrease in furfural yield was observed when catalysts with higher catalytic activities were used for biomass pretreatment under more severe conditions.

4. Techno-economy and green assessments for furfural production

A techno-economic assessment of furfural production involves considering the production technology options, total costs, and profit evaluation. Production technologies (pretreatment, extraction, and production facilities) are crucial for optimizing the production of products. The total costs consist of a fixed capital investment (cost of new-plant construction), direct costs (external battery and the total costs of purchasing and installing all process equipment), indirect costs (legal expenses, construction costs, and contractor fees), operating costs (variable and fixed costs, raw materials, and utility costs), and working capital (cost needed to start and run a plant until it generates sufficient revenue to pay off debt and purchase inventory).[134] The variable operating costs (feedstocks, raw materials, waste handling, and byproduct credits) were determined based on the Aspen Plus process modeling results, and prices were obtained from prior studies.[135] The fixed operating capital (employee salaries, labor burden, maintenance, and property insurance) was estimated following the assumptions of the NREL TEA report.[136]

The economic metrics commonly used to evaluate the economic performance of a biorefinery include the internal rate of

return (IRR), return on investment (ROI), net present value (NPV), earnings before interest, taxes, depreciation, amortization (EBITDA), resistance to market uncertainty (RTMU), return on capital employed (ROCE), payback period (PP), and annualized investment cost (EAC).[137] Usually, a sensitivity analysis provides a better idea of the risks and RTMU of different biorefinery inputs. The reported techno-economic assessments of different biorefinery options were reviewed in detail.

4.1. Techno-economy assessment for furfural and co-product production

Integrated production of furfural and glucose. Mohammed *et al.*[134] developed a profitable integrated process plant that produced glucose and furfural from empty palm oil fruit bunches. The number of stages in the distillation column, reflux ratio, solvent type (butyl chloride or toluene), and recycling flow rate were evaluated to maximize the yield and purity of the products. The findings indicated that the optimal number of stages ranged from 2 to 10, and the reflux ratio was 0.9. The optimal flow rate was 34.86 kg h^{-1}, and butyl chloride was selected as the solvent for the furfural production unit. For the economic analysis, the calculated FCI, direct cost, indirect cost, annual operating capital and working capital were 20.80 million USD, 15.16 million USD, 5.65 million USD, 1138.66 million USD per ton, and 3.74 million USD, respectively. The techno-economic findings after the profitability evaluation indicated that the project can successfully achieve an NPV of 7.65 million USD with a positive IRR of 14.25% and a ROI of 22.06% by summing the discounted cash flows after tax at a 10% discount rate over 23 years.

Integrated production of furfural and ethanol. Ntimbani *et al.*[138] compared self-sufficient furfural alone (scenario 1), ethanol alone (scenario 2), and the co-production of furfural and ethanol (scenarios 3–7) for the one-step furfural production. The results of the economic analysis are presented in Table 4. Considering scenarios 5 and 7, multi-product biorefineries were effective in hedging against the ethanol price fluctuations compared to ethanol production alone, and resulted in furfural yields of 68.73 and 50.47%, respectively; the furfural selling price dominantly contributed to 61–71% of the total revenue. Scenario 3, which demonstrated a furfural yield of only 14%, was the most effective in reducing exposure to the furfural price fluctuations and was more susceptible to the ethanol price fluctuations. The analysis results demonstrated that the biorefinery indicated by scenario 5 was the most profitable, regardless of the 25% decrease (ethanol or furfural) in the product price, compared to the production of ethanol (scenario 2) or furfural (scenario 1) alone.

The traditional one-stage and proposed two-stage steam-explosion pretreatments for the production of furfural integrated with the co-production of ethanol from sugarcane lignocelluloses were evaluated.[139] A sensitivity analysis showed that in terms of the product prices, the IRRs of the two-stage furfural-ethanol biorefineries were less sensitive to the furfural price fluctuations, whereas the one-step process had a higher furfural yield and lower ethanol yield, and the profitability was less dependent on the ethanol sales but more limited to higher production costs. Therefore, the total revenue from the co-production of furfural and ethanol of the two-step process was higher than that of the one-step steam-explosion (SE) process (170 °C and 0.5 wt% H_2SO_4). Additionally, varying severities of the steam explosion (scenarios 1, 2 and 3) were found to affect the two-step furfural revenue (Table 5). The biorefinery utilizing a pretreatment method with a medium severity level (Scenario 2) was considered more robust and economical owing to the high yields of both furfural and ethanol, demonstrated less volatile product prices, and lower investment costs owing to the reduced process intensification.

Integrated production of furfural, lignin, and ethanol. Zang *et al.*[135] evaluated the techno-economic feasibility of the one-pot simultaneous biomass pretreatment and furfural production using aqueous choline chloride (ChCl) and methyl isobutyl ketone (MIBK) systems. Considering seven process areas, the total capital investment (TCI), total variable operating cost (TVO), and the market price fluctuations of lignin, furfural, and ethanol are presented in Table 6. A sensitivity analysis demonstrated that the technical parameters (*e.g.*, reaction temperature and solid loading) had a larger effect on the minimum furfural selling price (MFSP) than the economic factors (*e.g.*, material cost and installation cost). According to the mass balance results, the yields of furfural, lignin, and ethanol from wet biomass per t were 109, 97, and 124 kg, respectively. Considering the lowest lignin price (250 $ per t) and ethanol selling price (1.75 $ per gal), the MFSP can reach the highest value (1115 $ per t), and with the lowest MFSP, the lignin price is (250 $ per t). The evaluation results suggest that

Table 5 Key economic results for investigated furfural and ethanol biorefineries from lignocellulose at 2018 cost year of analysis[138]

	TCI (million)	TCOP (million USS per year)	Ethanol yield (%)	IRR (%)	IRR (%)	IRR (%) without electricity credit
Scenario 1	272	13.7	59.50	—	12.92	9.91
Scenario 2	294	18.12	—	95.69	10.18	8.26
Scenario 3	327	18.37	13.68	63.79	3.64	−0.56
Scenario 4	306	18.17	31.14	74.71	74.71	3.99
Scenario 5	305	18.57	68.73	53.51	53.51	10.30
Scenario 6	305	18.17	29.00	77.3	77.30	5.8
Scenario 7	322	18.89	50.47	17.02	17.02	7.69
Scenario 5* (2015 cost year)	264	17.03	68.73	53.51	53.51	4.90

Table 6 Economic analysis of furfural and ethanol co-production[139]

Process description	TCI (US$)	TCOP (MILLION US$ per year)	Ethanol/dry feedstock (kg t^{-1})	FF/dry feedstock (kg t^{-1})	IRR (%)
Scenario 1 (SE at 190 °C, FF reactor at 180 °C with 2.0 wt% H_2SO_4)	322.58	20.20	150.2	78.1	13.11
Scenario 2 (SE at 205 °C, FF reactor at 180 °C with 2.0 wt% H_2SO_4)	310.23	19.85	213.8	90.6	13.59
Scenario 2 (SE at 215 °C, FF reactor at 180 °C with 2.0 wt% H_2SO_4)	340.46	20.74	156.3	46.4	10.07
One-step FF (170 °C and 0.5 wt% H_2SO_4) and ethanol	290.79	19.36	89.8	137.5	12.78

at least $\frac{1}{4}$ of the current plant scale (32 579 kg h^{-1}) can ensure a profitable system, and the MFSP can reach 945 $ per t. The techno-economic analysis results suggest that the proposed system with diverse market-driven products is cost-competitive and has a low economic risk.

Co-production of furfural and levoglucosenone. Halder *et al.*[140] presented a techno-economic analysis of the pyrolysis of ionic liquid choline glycinate ([Ch][Gly]) pre-treated sugarcane straw (SCS) for the co-production of furfural and levoglucosenone (LGO). The mass balance results demonstrated that using [Ch][Gly] fractioned the lignocellulosic structure and resulted in approximately 14.4 and 3.6% of furfural and LGO, respectively. The sensitivity analysis results of different factors indicated that solid loading had a larger impact on the furfural and LGO production cost; the net production costs of furfural and LGO were estimated to be approximately 0.75 AU$ per kg and 0.05 AU$ per kg, respectively. IL recycling had a greater impact on the NPV and PP at lower biomass loadings. The increase in the capital cost, tax rate, interest rate, and IL cost reduced the NPV and increased the PP. The NPV linearly increased in the integrated biorefinery process as the plant size increased, whereas the MSP of furfural and LGO decreased nonlinearly. The base-case analysis, including the heat recovery, capital cost, interest rate, furfural yield, LGO yield, IL recycling, and IL cost, suggested that the plant (1150 kg h^{-1}) would produce approximately 6.9 MAU$ net benefits after 30 years, with a PP of 15.4 years.

Overall, the integrated biorefinery for the co-production of furfural and other products would ensure robust revenues by maximizing feedstock utilization. The results of this economic analysis are encouraging for the scale-up process development.

4.2. Green evaluation

Biorefineries for furfural production should comply with the concept of "Green Chemistry". For achieving techno-economic efficiency, green and sustainable production processes should avoid using toxic and hazardous materials, instead green solvents and catalysts should be selected to, reduce the energy input and, waste yields; furthermore, recycling technology should be applied for reusing catalysts, solvents, and waste water, and to operate waste-water treatment.

Solvent selection. Nhien *et al.*[141] evaluated the techno-economics of hybrid extraction and distillation processes for furfural separation and purification from vapor stream after the hydrolysis of lignocellulose biomass. The effectiveness of ten selected potential solvents was investigated, and the three best solvents (toluene, benzene, and butyl chloride) were designed and optimized. The results demonstrated that benzene was the most suitable solvent for furfural production. However, benzene is toxic; therefore, butyl chloride was proposed as a good choice for the hybrid purification of furfural; it can achieve total annual cost savings of up to 44.7% and demonstrates lower total annual CO_2 emissions (26.7) compared to benzene solvents.

IL and catalyst regeneration. Viar *et al.*[142] presented the techno-economic analyses of furan (furfural and 5-hydroxymethylfurfural) production from mixed sugar hydrolysates *via* a novel hybrid enzyme-chemocatalytic process. A cost comparison of scenarios I–IV is presented in Table 7. Scenario I was a multi-step process for furfural production, including simultaneous isomerization and reactive extraction (SIRE), back extraction (BE), and dehydration, with an initial mixed-sugar concentration of 40 g L^{-1}. In scenario II, a mixed sugar hydrolysate with a concentration of 160 g L^{-1} was used as the feed. Because THF contributes to the high energy and capital costs of the dehydration reactor, scenario III applied alternative methods (air/gas stripping-based entrainer-intensified vacuum reactive distillation) for furan recovery. Scenario IV considered the regeneration of HCl and NaOH for reuse rather than undergoing wastewater treatment. The assessment results demonstrated that the integration of novel technologies in furan–IL separation, energy-efficient furan recovery, and acid/base regeneration can effectively reduce the net cost of raw materials from $174 to $127MM. Sensitivity analyses identified modest improvements (10%) in the cost of feed stock sugar; the overall furan yield can reduce the minimum furan selling price to $1.23 per kg, which is competitive for fuel and polymer precursor applications.

Energy integration process. The energy integration process was green and economically feasible. Moncada *et al.*[143] investigated the technical, economic, and environmental performance of ethanol and furfural production from *Pinus patula* bark. Three scenarios were considered: (i) non-integrated process (scenario 1), (ii) full-energy integration process (scenario 2), and (iii) fully-integrated process with a cogeneration scheme (scenario 3). The economic analysis results of scenarios 1–3 are shown in Table 8, suggesting that compared to scenario 1, the heating and cooling utilities in scenario 2 decreased by 59% and 47%, respectively, and the remaining 92% of the heating utilities were covered by steam generated from the cogeneration process (scenario 3). The results of the economic evaluation demonstrate that scenario 3 had a higher NPV (128%) compared to scenario 2 owing to the fact that it had the lowest annualized production costs and highest

Table 7 Economic evaluation of process costs and profits[135]

Process area and profit		Equipment installation cost (million $)		Variable operating cost (million $ per year)		Market price
Process area	Feedstock handling	32.6		63.1		
	Biomass fractionation	67.0	One-pot reactor (17.1% of TCI) Distillers (3.1% of TCI) Separators (2.5% of TCI)	57.7	Feedstock cost shares (40.6% of TVC) ChCl (19.7% of TVC) MIBK and acetone (7.1% and 8.9% of TVC)	
	Cellulose conversion	61.8	Bioreactors (8.3% of TCI) Rectification columns (5.9% of TEIC)	2.3		
	Turbine and boiler	38.4		1.0		
	Enzyme production	21.7		13.7		
	Wastewater treatment	38.0		3.0		
	Storage and utilities	10.5		0.2		
Waste disposal		0.8				
Grid electricity		13.8				
Total variable operating cost		155.6				
Fixed operating cost		13.0				
Profit	Products					Ethanol: 1.75–4.15 $ per gal Lignin: 250–750 $ per t Furfural: around 1000 $ per t in 2017
	Plant scale					When it is downscaled to 32 579 kg h^{-1} ($\frac{1}{4}$ of the current design), the minimum furfural selling price increases up to 945 $ per t

Table 8 The cost assessment of scenario I–IV[142]

Scenario	Total capital cost (MM$)	Cost of raw material (MM$)	Cost of thermal utility (MM$)	Cost of electricity (MM$)	Total operating cost (MM$)	MFSP $ per kg
I	296.1	187.2	74.4	1.3	264.6	2.40
II	239.9	187.2	71.3	0.9	261	2.26
III	113	174.2	12.6	11.5	199.9	1.60
IV	120.7	127.6	12.6	30.1	171.9	1.42

annualized product revenues, and this scenario was the least economically feasible. Regarding scenario 3, the results of the sensitivity analysis revealed that the NPV value was mainly affected by the furfural and ethanol prices, and this scenario can suffer economic losses if the furfural prices decrease by over 73%. Overall, scenario 3, with a fired cogeneration system considering energy integration, allows for an increase in the economic income and decreases the potential environmental impacts.

Similarly, Mazar *et al.*[144] conducted a techno-economic evaluation to quantify the performance of alternative process configurations. The results showed that significant heat energy savings (99.5%) were achieved in driving the process using a heat exchanger network designed for internal heat recovery, and even the processes with the lowest performance would be profitable, robust, and capital-efficient. In addition, a process for heat integration was reported by Clauser *et al.* and Hernández *et al.* Clauser *et al.*[145] proposed the co-production of carboxylic acids, furfural, and pellets in a pine sawdust biorefinery. Three alternatives for the conversion of residual solids were analyzed: (i) use of 100% of the residual solid for pellet production (alternative I); (ii) use of residual solid for the production of steam and 34 kg of pellets, and obtained steam for reuse (alternative II); (iii) use of residual solid for the production of steam and 105 kg of pellets with all process heat integration for reuse (alternative III). The economic results of three studied biorefinery scenarios are presented in Table 9. The results demonstrated that alternative I consumed more energy than alternative II, and alternative III consumed more energy with the heat integration process; a higher pellet yield

Table 9 Annualized production costs and revenues of three scenarios[143]

	Scenario 1		Scenario 2		Scenario 3	
Categories	M.USD per y	Share (%)	M.USD per y	Share (%)	M.USD per y	Share (%)
Annualized production costs						
Raw materials	36.57	30.96	36.57	42.28	36.67	53.99
Utilities	71.01	60.12	33.98	39.30	11.49	16.92
Maintenance	2.38	2.02	3.72	4.30	4.60	6.77
Labor	0.51	0.43	0.51	0.59	0.67	0.98
Fixed and general	1.2	1.02	1.82	2.10	2.26	3.32
Overhead	1.52	1.28	2.21	2.56	2.75	4.05
Capital depreciation	4.92	4.17	7.67	8.87	9.49	13.97
Total costs	118.12	100	86.48	100	67.92	100
Revenues						
Ethanol	48.06	41.33	48.06	41.33	48.06	37.87
Furfural	68.22	58.67	68.22	58.67	68.22	53.76
Electricity	0	0	0	0	10.61	8.36
Total revenue	116.28	100	116.28	100	126.89	100
Economic metrics						
NPV (M.USD per y)	−31.53		80.90		184.54	
Payout period (y)	Larger than project's life time		3.41		2.22	

Table 10 The economic results of three studied biorefinery scenarios[144]

				Production costs	
Alternative	Option	IRR (%)	Investment (MUSD[a])	Pellets (USD per ton)	LA (USD per kg)[b]
I		13.4	75.0	62.42	3.71
II	(a)	16.5	70.5	132.04	2.57
	(b)	16.6	70.1	—	2.57
III		17.0	71.7	76.14	2.54

[a] Millions of USD. [b] The production costs of LA include the production costs of FA and furfural. Alternative II-a (the use of a fraction of the pre-treated sawdust for steam production); alternative II-b without any pellet production.

Table 11 Annualized costs for each scenario

	Base case		Scenarios 1		Scenarios 2	
Item	Million US$ per year	Share (%)	Million US$ per year	Share (%)	Million US$ per year	Share (%)
Depreciation of capital	1.765	4	2.166	4	2.815	4
Raw material			11.4911	19	11.491	16
Utilities	20.670	45	14.789	24	18.818	27
Operating	23.867	52	31.916	53	36.765	53
Total	46.302		60.363		69.880	

resulted in a high IRR owing to the high market value of levulinic acid (LA) (5–9 USD per kg) and the low cost investment.

Hernández *et al.*[146] evaluated three techno-economic scenarios: (1) the base case considered power production through a direct combustion process at 850 °C and 60 bar; (2) scenario 1 considered production of xylitol, furfural, ethanol and poly-3-hydroxybutyrate PHB; (3) scenario 2 utilized the solid residues resulting from xylitol, furfural, ethanol and PHB processes for producing power and heat through a cogeneration system (Table 10). Results indicated that despite the co-production of xylitol, furfural, ethanol, and PHB integrated into a cogeneration system for producing power and heat from the solid residues increased total cost, the feasibility was positive with a profit margin of 53% and resulted in a lower contamination level regarding the environmental analysis (Table 11).

5. Future research outlook

5.1 Integrated biorefinery process for furfural production

An integrated strategy for furfural production has considerable potential to capitalize on all three primary components (cellulose, hemicellulose, and lignin) of lignocellulosic biomass. One- and two-step methods for the selective separation of hemicellulose and subsequent furfural production are required to ensure residue solids for further reuse. Designs for

zero-waste manufacturing and waste management sectors can be obtained by reusing and recycling techniques.

5.2 Cost-saving and economic sustainability

Recycling solvents and catalysts is an effective solution for achieving cost savings. Modern assisted pretreatment technologies, such as ultrasound, are novel green technologies that can effectively break down plant cells and reduce energy consumption. Liquid–liquid extraction is also energy-efficient for extraction and separation in a biphasic system. One- and two-step approaches for the separation of hemicellulose and lignin require more initial energy input than the selective separation of hemicellulose in dilute acid-catalyzed systems. Therefore, recycling and economical DES with low-cost metal salts at mild temperatures for cost-saving furfural production need to be further explored. In addition, future engineers should focus on the design of heat-capture equipment for energy collection to reduce the considerable electrical costs. Installing water recycling pipes, decreasing water consumption, and using waste water treatment systems are necessary for economic sustainability.

5.3 Green technologies for improving furfural selectivity and yield

Furfural has been identified as one of the key 'green' chemicals produced in the so-called lignocellulosic feedstock biorefinery.[147] Furfural is easily degraded into unwanted products in water. Biphasic systems with organic solvents as the extraction layer, such as MIBK/H_2O and GVL/H_2O systems, have been proven to enhance the furfural yield by minimizing undesired furfural degradation reactions. GVL is considered a promising green solvent and is effective for furfural production and lignin solutions. The use of traditional toxic inorganic acids as catalysts for furfural production is undesired; therefore, widely applied alternative green catalysts for large-scale integrated processes are more attractive.

6. Conclusion

Agricultural waste is rich in xylan-type hemicellulose and is regarded as the best raw material for furfural production. The one-step process can directly convert biomass to furfural, whereas the two-step process requires the additional separation of pentose-rich hydrolysate, which is further converted to furfural under severe pretreatment conditions. Organic solvents and catalysts are important operating variables in the one- and two-step production of furfural. The selection of appropriate catalysts and organic solvents can effectively improve the yield and selectivity of furfural. The hydrogen ions provided by the catalyst promote the hydrolysis of hemicellulose, the presence of chloride ions accelerates the production rate of furfural, and biphasic solvent systems effectively prevent the degradation of furfural. The emerging DESs and ILs are expected to contribute to the utilization of integrated biomass resources. The industrialization of furfural requires a techno-economic evaluation of the entire process of furfural production, and the best production scheme is determined by evaluating the total cost and profit to ensure a stable profit. The integrated biorefinery strategy for the co-production of furfural and ethanol or 5-hydroxymethylfurfural is more economical than the biomass refining strategy for the production of furfural alone. Future developments will be directed towards greener and more cost-effective furfural production strategies.

Author contributions

Yuqi Bao: conceptualization and writing – review and editing; Zicheng Du and Xiaoying Liu: investigation and writing – original draft; Chengrong Qin: funding acquisition and resources; Hui Liu and Jinsong Tang: validation; Caoxing Huang and Chen Liang: formal analysis; Shuangquan Yao: project administration and supervision.

Conflicts of interest

The authors declare that they have no known competing financial interests or personal relationships that could have appeared to influence the work reported in this paper.

Acknowledgements

This work was sponsored by the National Key Research and Development Program (2022YFC2105505). This project was supported by the Guangxi Natural Science Foundation of China (2023GXNSFGA026001).

References

1 Y. Zhao, K. Lu, H. Xu, L. Zhu and S. Wang, *Renewable Sustainable Energy Rev.*, 2021, **139**, 110706.
2 Y. Zhuang, Z. Si, S. Pang, H. Wu, X. Zhang and P. Qin, *J. Cleaner Prod.*, 2023, **396**, 136481.
3 W. Deng, Y. Feng, J. Fu, H. Guo, Y. Guo, B. Han, Z. Jiang, L. Kong, C. Li, H. Liu, P. T. T. Nguyen, P. Ren, F. Wang, S. Wang, Y. Wang, Y. Wang, S. S. Wong, K. Yan, N. Yan, X. Yang, Y. Zhang, Z. Zhang, X. Zeng and H. Zhou, *Green Energy Environ.*, 2023, **8**, 10–114.
4 S. Zhang, M. C. Chi, J. L. Mo, T. Liu, Y. H. Liu, Q. Fu, J. L. Wang, B. Luo, Y. Qin, S. F. Wang and S. X. Nie, *Nat. Commun.*, 2022, **13**, 4168.
5 S. X. Nie, C. J. Chen and C. J. Zhu, *Front. Chem. Sci. Eng.*, 2023, **17**, 795–797.
6 C. B. T. L. Lee and T. Y. Wu, *Renewable Sustainable Energy Rev.*, 2021, **137**, 110172.
7 Y. Lu, Q. He, G. Fan, Q. Cheng and G. Song, *Green Process. Synth.*, 2021, **10**, 779–804.

8 S. G. C. Almeida, G. F. Mello, T. K. Kovacs, D. D. V. Silva, M. A. M. Costa and K. J. Dussán, *Waste Biomass Valorization*, 2022, **13**, 4013–4025.
9 M. S. N. Sai, D. De and B. Satyavathi, *J. Cleaner Prod.*, 2021, **327**, 129467.
10 A. Wang, N. P. Balsara and A. T. Bell, *Green Chem.*, 2018, **20**, 2903–2912.
11 M. Yazdizadeh, M. R. J. Nasr and A. Safekordi, *RSC Adv.*, 2016, **6**, 55778–55785.
12 M. C. Chi, S. Zhang, T. Liu, Y. H. Liu, B. Luo, J. L. Wang, C. C. Cai, X. J. Meng, S. F. Wang, Q. S. Duan and S. X. Nie, *Adv. Funct. Mater.*, 2024, **34**, 2310280.
13 V. Aristizábal-Marulanda, J. A. Poveda-Giraldo and C. A. Cardona Alzate, *Sci. Total Environ.*, 2020, **728**, 138841.
14 B. Qiu, J. Shi, W. Hu, J. Gao, S. Li and H. Chu, *Fuel*, 2023, **354**, 129278.
15 K. J. Yong, T. Y. Wu, C. B. T. L. Lee, Z. J. Lee, Q. Liu, J. M. Jahim, Q. Zhou and L. Zhang, *Biomass Bioenergy*, 2022, **161**, 106458.
16 C. Feng, J. Zhu, Y. Hou, C. Qin, W. Chen, Y. Nong, Z. Liao, C. Liang, H. Bian and S. Yao, *Bioresour. Technol.*, 2022, **348**, 126793.
17 H. Zeng, B. Liu, J. Li, M. Li, M. Peng, C. Qin, C. Liang, C. Huang, X. Li and S. Yao, *Bioresour. Technol.*, 2022, **351**, 126951.
18 L. C. Nhien, N. V. D. Long and M. Lee, *Energy*, 2021, **14**, 1152.
19 T. Heinze, L. H. Skodda and M. Gericke, *Carbohydr. Polym.*, 2023, **300**, 120251.
20 Y. Li, M. Yao, Y. Luo, J. Li, Z. Wang, C. Liang, C. Qin, C. Huang and S. Yao, *ACS Appl. Mater. Interfaces*, 2023, **15**, 5883–5896.
21 J. Rao, Z. Lv, G. Chen and F. Peng, *Prog. Polym. Sci.*, 2023, **140**, 101675.
22 C. Huang, B. Jeuck, J. Du, Q. Yong, H. M. Chang, H. Jameel and R. Phillips, *Bioresour. Technol.*, 2016, **219**, 600–607.
23 J. Li, B. Liu, L. Liu, Y. Luo, F. Zeng, C. Qin, C. Liang, C. Huang and S. Yao, *Bioresour. Technol.*, 2023, **376**, 128855.
24 L. Liu, B. Liu, X. Li, Z. Wang, L. Mu, C. Qin, C. Liang, C. Huang and S. Yao, *Ind. Crops Prod.*, 2023, **200**, 116811.
25 C. H. Lai, Y. Jia, C. D. Yang, L. W. Chen, H. Shi and Q. Yong, *ACS Sustainable Chem. Eng.*, 2020, **8**, 1797–1804.
26 T. Zhang, W. Li, Z. Xu, Q. Liu, Q. Ma, H. Jameel, H. M. Chang and L. Ma, *Bioresour. Technol.*, 2016, **209**, 108–114.
27 E. Cousin, K. Namhaed, Y. Pérès, P. Cognet, M. Delmas, H. Hermansyah, M. Gozan, P. A. Alaba and M. K. Aroua, *Sci. Total Environ.*, 2022, **847**, 157599.
28 B. Liu, L. Liu, X. Qin, Y. Liu, R. Yang, X. Mo, C. Qin, C. Liang and S. Yao, *Int. J. Mol. Sci.*, 2023, **24**, 11809.
29 Y. Luo, B. Liu, B. Deng, X. Long, Z. Du, C. Qin, C. Liang, C. Huang and S. Yao, *Ind. Crops Prod.*, 2024, **208**, 117791.
30 R. Bielski and G. Grynkiewicz, *Green Chem.*, 2021, **23**, 7458–7487.
31 Y. Lee, S. W. Lee, Y. F. Tsang, Y. T. Kim and J. Lee, *Chem. Eng. J.*, 2020, **387**, 124194.
32 Z. Zhang, Z. Pei, H. Chen, K. Chen, Z. Hou, X. Lu, P. Ouyang and J. Fu, *Ind. Eng. Chem. Res.*, 2018, **57**, 4225–4230.
33 J. M. Guo, K. X. Huang, S. Z. Zhang and Y. Xu, *J. Chem. Technol. Biotechnol.*, 2020, **95**, 475–884.
34 A. Kumar, A. S. Chauhan, R. Bains and P. Das, *Green Chem.*, 2023, **25**, 849–870.
35 P. Y. Wen, T. Zhang, L. T. Wei, J. Y. Wang, A. J. Ragauskas, Y. Zhang, Y. Xu and J. Zhang, *ACS Sustainable Chem. Eng.*, 2021, **9**, 11361–11371.
36 R. Gérardy, D. P. Debecker, J. Estager, P. Luis and J.-C. M. Monbaliu, *Chem. Rev.*, 2020, **120**, 7219–7347.
37 S. Takkellapati, T. Li and M. A. Gonzalez, *Clean Technol. Environ. Policy*, 2018, **20**, 1615–1630.
38 Y. Q. Sheng, Y. Zhang, H. Z. Ma, Y. Xu and M. B. Tu, *ACS Sustainable Chem. Eng.*, 2020, **8**, 7892–7900.
39 J. Li, T. Li, Y. Wang, Z. Du, Y. Luo, C. Qin, C. Liang, C. Huang and S. Yao, *Ind. Crops Prod.*, 2023, **205**, 117453.
40 D. Fan, X. Xie, C. Li, X. Liu, J. Zhong, X. Ouyang, Q. Liu and X. Qiu, *J. Agric. Food Chem.*, 2021, **69**, 10838–10847.
41 J. L. Wen, S. L. Sun, B. L. Xue and R. C. Sun, *J. Agric. Food Chem.*, 2013, **61**, 635–645.
42 L. Fang, Y. Su, P. Wang, C. Lai, C. Huang, Z. Ling and Q. Yong, *Bioresour. Technol.*, 2022, **348**, 126795.
43 J. Han, R. Cao, X. Zhou and Y. Xu, *Bioresour. Technol.*, 2020, **307**, 123200.
44 W. J. Xu, S. P. Zhang, J. J. Lu and Q. J. Cai, *Environ. Prog. Sustainable Energy*, 2017, **36**, 690–695.
45 P. Alvira, M. J. Negro, I. Ballesteros, A. González and M. J. B. Ballesteros, *Bioethanol*, 2016, **1**, 66–75.
46 F. Wang, B. Liu, W. Cao, L. Liu, F. Zeng, C. Qin, C. Liang, C. Huang and S. Yao, *Bioresour. Technol.*, 2023, **385**, 129416.
47 Y. Hou, S. Wang, B. Deng, Y. Ma, X. Long, C. Qin, C. Liang, C. Huang and S. Yao, *Int. J. Biol. Macromol.*, 2023, **251**, 126374.
48 C. Sawatdeenarunat, K. C. Surendra, D. Takara, H. Oechsner and S. K. Khanal, *Bioresour. Technol.*, 2015, **178**, 178–186.
49 L. Zhang, W. Zhang, F. Zhang and J. Jiang, *Bioresour. Technol.*, 2021, **341**, 125897.
50 X. Zhou, J. Zhao, X. Zhang and Y. Xu, *Bioresour. Technol.*, 2019, **289**, 121755.
51 I. Kim, B. Lee, J. Y. Park, S. A. Choi and J. I. Han, *Carbohydr. Polym.*, 2014, **99**, 563–567.
52 J. Liang, B. Liu, X. Li, X. Mo, C. Qin, C. Liang, C. Huang and S. Yao, *Bioresour. Technol.*, 2023, **384**, 129328.
53 M. H. Chen, M. J. Bowman, M. A. Cotta, B. S. Dien, L. B. Iten, T. R. Whitehead, K. D. Rausch, M. E. Tumbleson and V. Singh, *Carbohydr. Polym.*, 2016, **140**, 96–103.

54 S. Ge, Y. Wu, W. Peng, C. Xia, C. Mei, L. Cai, S. Q. Shi, C. Sonne, S. S. Lam and Y. F. Tsang, *Chem. Eng. J.*, 2020, **385**, 123949.
55 M. Ebrahimi, O. B. Villaflores, E. E. Ordono and A. R. Caparanga, *Bioresour. Technol.*, 2017, **228**, 264–271.
56 B. Palmarola-Adrados, M. Galbe and G. Zacchi, *J. Chem. Technol. Biotechnol.*, 2005, **80**, 85–91.
57 S. Wang, B. Liu, J. Liang, F. Wang, Y. Bao, C. Qin, C. Liang, C. Huang and S. Yao, *Bioresour. Technol.*, 2023, **382**, 129154.
58 Q. A. Yu, X. S. Zhuang, Z. H. Yuan, W. Qi, Q. O. Wang and X. S. Tan, *Bioresour. Technol.*, 2011, **102**, 3445–3450.
59 H. Lyu, J. Zhang, J. Zhou, X. Shi, C. Lv and Z. Geng, *Fuel Process. Technol.*, 2019, **195**, 106148.
60 J. N. M. Soetedjo, C. B. Rasrendra and H. J. Heeres, *IOP Conf. Ser.: Mater. Sci. Eng.*, 2020, **742**, 012049.
61 T. A. Natsir and S. Shimazu, *Fuel Process. Technol.*, 2020, **200**, 106308.
62 H. Huang, Z. Li, Y. Ma, M. Yao and S. Yao, *Carbohydr. Polym.*, 2023, **303**, 120461.
63 Y. You, X. Zhang, P. Li, F. Lei and J. Jiang, *Bioresour. Technol.*, 2020, **306**, 123131.
64 W. Zhang, Y. You, F. Lei, P. Li and J. Jiang, *Bioresour. Technol.*, 2018, **265**, 387–393.
65 B. Danon, G. Marcotullio and W. de Jong, *Green Chem.*, 2014, **16**, 39–54.
66 G. Marcotullio and W. De Jong, *Green Chem.*, 2010, **12**, 1739–1746.
67 L. Y. Mao, L. Zhang, N. B. Gao and A. M. Li, *Green Chem.*, 2013, **15**, 727–737.
68 D. Ouyang, T. Liu, A. A. Astimar, H. L. N. Lau, S. S. Teh, J. Nursyairah, D. Liu and X. Zhao, *Bioresour. Technol.*, 2023, **372**, 128626.
69 Z. Chen, X. Bai, A. Lusi, W. A. Jacoby and C. Wan, *Bioresour. Technol.*, 2019, **289**, 121708.
70 E. Z. Hoşgün, *Biomass Convers. Biorefin.*, 2021, **11**, 2703–2710.
71 J. Ren, W. Wang, Y. Yan, A. Deng, Q. Chen and L. Zhao, *Cellulose*, 2016, **23**, 1649–1661.
72 C. M. Cai, N. Nagane, R. Kumar and C. E. Wyman, *Green Chem.*, 2014, **16**, 3819–3829.
73 L. Zhang, H. Yu, P. Wang, H. Dong and X. Peng, *Bioresour. Technol.*, 2013, **130**, 110–116.
74 Y. Li, L. L. Sun, D. M. Cao, X. F. Cao and S. N. Sun, *Bioresour. Technol.*, 2023, **386**, 129520.
75 X. Li, Q. Liu, C. Si, L. Lu, C. Luo, X. Gu, W. Liu and X. Lu, *Ind. Crops Prod.*, 2018, **120**, 343–350.
76 I. Harry, H. Ibrahim, R. Thring and R. Idem, *Biomass Bioenergy*, 2014, **71**, 381–393.
77 O. Ogundowo, G. Sadanandam and H. Ibrahim, *React. Kinet., Mech. Catal.*, 2023, **136**, 2535–2554.
78 X. Li, X. Lu, W. Hu, H. Xu, J. Chen, J. Xiong, L. Lu, Z. Yu and C. Si, *Fuel Process. Technol.*, 2022, **229**, 107178.
79 C. X. Jiang, J. H. Di, C. Su, S. Y. Yang, C. L. Ma and Y. C. He, *Bioresour. Technol.*, 2018, **268**, 315–322.
80 D. Cai, H. Chen, C. Zhang, X. Teng, X. Li, Z. Si, G. Li, S. Yang, G. Wang and P. Qin, *J. Cleaner Prod.*, 2021, **283**, 125410.
81 P. Liu, S. Shi, L. Gao and G. Xiao, *React. Kinet., Mech. Catal.*, 2022, **135**, 795–810.
82 Y. Chen, Y. Zhou, R. Zhang and C. Hu, *Mol. Catal.*, 2020, **484**, 110729.
83 Y. Bao, J. Zhu, F. Zeng, J. Li, S. Wang, C. Qin, C. Liang, C. Huang and S. Yao, *Bioresour. Technol.*, 2022, **364**, 128082.
84 O. Yemis and G. Mazza, *Bioresour. Technol.*, 2011, **102**, 7371–7378.
85 X. Li, J. Yang, R. Xu, L. Lu, F. Kong, M. Liang, L. Jiang, S. Nie and C. Si, *Ind. Crops Prod.*, 2019, **135**, 196–205.
86 T. Zhang, W. Li, S. An, F. Huang, X. Li, J. Liu, G. Pei and Q. Liu, *Bioresour. Technol.*, 2018, **264**, 261–267.
87 P. Brazdausks, A. Paze, J. Rizhikovs, M. Puke, K. Meile, N. Vedernikovs, R. Tupciauskas and M. Andzs, *Biomass Bioenergy*, 2016, **89**, 98–104.
88 L. Zhu, X. Shao, X. Pan, Z. Sun, X. Li, X. Duan and J. Shi, *Biomass Bioenergy*, 2023, **171**, 106734.
89 X. Teng, Z. Si, S. Li, Y. Yang, Z. Wang, G. Li, J. Zhao, D. Cai and P. Qin, *Ind. Crops Prod.*, 2020, **151**, 112481.
90 X. K. Li, Z. Fang, J. Luo and T. C. Su, *ACS Sustainable Chem. Eng.*, 2016, **4**, 5804–5813.
91 Z. Zhou, D. Liu and X. Zhao, *Renewable Sustainable Energy Rev.*, 2021, **146**, 111169.
92 K. Dussan, B. Girisuta, M. Lopes, J. J. Leahy and M. H. B. Hayes, *ChemSusChem*, 2015, **8**, 1411–1428.
93 J. C. Solarte-Toro, J. M. Romero-García, J. C. Martínez-Patiño, E. Ruiz-Ramos, E. Castro-Galiano and C. A. Cardona-Alzate, *Renewable Sustainable Energy Rev.*, 2019, **107**, 587–601.
94 Q. Wang, X. Zhuang, W. Wang, X. Tan, Q. Yu, W. Qi and Z. Yuan, *Chem. Eng. J.*, 2018, **334**, 698–706.
95 X. Li, Q. Liu, C. Luo, X. Gu, L. Lu and X. Lu, *ACS Sustainable Chem. Eng.*, 2017, **5**, 8587–8593.
96 S. Jiang, C. Verrier, M. Ahmar, J. Lai, C. Ma, E. Muller, Y. Queneau, M. Pera-Titus, F. Jérôme and K. De Oliveira Vigier, *Green Chem.*, 2018, **20**, 5104–5110.
97 W. Wang, J. Ren, H. Li, A. Deng and R. Sun, *Bioresour. Technol.*, 2015, **183**, 188–194.
98 Y. P. Luo, Z. Li, Y. N. Zuo, Z. S. Su and C. W. Hu, *ACS Sustainable Chem. Eng.*, 2017, **5**, 8137–8147.
99 Q. Qing, Q. Guo, L. Zhou, Y. Wan, Y. Xu, H. Ji, X. Gao and Y. Zhang, *Bioresour. Technol.*, 2017, **226**, 247–254.
100 X. Lyu and G. G. Botte, *Chem. Eng. J.*, 2021, **403**, 126271.
101 C. Liu, L. Wei, X. Yin, X. Pan, J. Hu, N. Li, J. Xu, J. Jiang and K. Wang, *Chem. Eng. J.*, 2021, **425**, 130608.
102 Z. K. Wang, X. J. Shen, J. J. Chen, Y. Q. Jiang, Z. Y. Hu, X. Wang and L. Liu, *Int. J. Biol. Macromol.*, 2018, **117**, 721–726.
103 C. B. T. L. Lee, T. Y. Wu, K. J. Yong, C. K. Cheng, L. F. Siow and J. M. Jahim, *Sci. Total Environ.*, 2022, **827**, 154049.
104 S. Peleteiro, V. Santos, G. Garrote and J. C. Parajó, *Carbohydr. Polym.*, 2016, **146**, 20–25.

105 L. Zhang, L. Tian, R. Sun, C. Liu, Q. Kou and H. Zuo, *Bioresour. Technol.*, 2019, **276**, 60–64.
106 J. Gao, H. Wang, X. Cao, Z. Li, H. Guo, X. Yang, W. Wang, N. Guo and Y. Ma, *Mol. Catal.*, 2023, **535**, 112890.
107 O. Ogundowo and H. Ibrahim, *Biomass Convers. Biorefin.*, 2024, **14**, 7743–7751.
108 R. Sirohi, J. P. Pandey, A. Singh, R. Sindhu, U. C. Lohani, R. Goel and A. Kumar, *Ind. Crops Prod.*, 2020, **149**, 112351.
109 H. Li, X. Wang, C. Liu, J. Ren, X. Zhao, R. Sun and A. Wu, *Ind. Crops Prod.*, 2016, **94**, 721–728.
110 S. Xiong, C. Luo, Z. Yu, N. Ji, L. Zhu and S. Wang, *Green Chem.*, 2021, **23**, 8458–8467.
111 R. L. Johnson, F. A. Perras, M. P. Hanrahan, M. Mellmer, T. F. Garrison, T. Kobayashi, J. A. Dumesic, M. Pruski, A. J. Rossini and B. H. Shanks, *ACS Catal.*, 2019, **9**, 11568–11578.
112 D. Scholz, O. Kröcher and F. Vogel, *ChemSusChem*, 2018, **11**, 2189–2201.
113 G. S. Foo, A. H. Van Pelt, D. Krötschel, B. F. Sauk, A. K. Rogers, C. R. Jolly, M. M. Yung and C. Sievers, *ACS Sustainable Chem. Eng.*, 2015, **3**, 1934–1942.
114 J. Wang, B. C. Lin, Q. X. Huang, Z. Y. Ma, Y. Chi and J. H. Yan, *Energy Fuels*, 2017, **31**, 11681–11689.
115 W. Sangarunlert, P. Piumsomboon and S. Ngamprasertsith, *Korean J. Chem. Eng.*, 2007, **24**, 936–941.
116 D. W. Rackemann, J. P. Bartley, M. D. Harrison and W. O. S. Doherty, *RSC Adv.*, 2016, **6**, 74525–74535.
117 A. R. C. Morais, M. D. D. J. Matuchaki, J. Andreaus and R. Bogel-Lukasik, *Green Chem.*, 2016, **18**, 2985–2994.
118 C. B. T. L. Lee, T. Y. Wu, C. H. Ting, J. K. Tan, L. F. Siow, C. K. Cheng, J. Md. Jahim and A. W. Mohammad, *Bioresour. Technol.*, 2019, **278**, 486–489.
119 E. S. Kim, S. Liu, M. M. Abu-Omar and N. S. Mosier, *Energy Fuels*, 2012, **26**, 1298–1304.
120 A. Deng, J. Ren, H. Li, F. Peng and R. Sun, *RSC Adv.*, 2015, **5**, 60264–60272.
121 Z. Chen, W. D. Reznicek and C. Wan, *ACS Sustainable Chem. Eng.*, 2018, **6**, 6910–6919.
122 M. Hu, Y. Yu and Y. Liu, *Ind. Crops Prod.*, 2023, **204**, 117334.
123 L. Penín, M. López, V. Santos and J. C. Parajó, *Molecules*, 2022, **27**, 4258.
124 W. C. Li, S. J. Zhang, T. Xu, M. Q. Sun, J. Q. Zhu, C. Zhong, B. Z. Li and Y. J. Yuan, *Energy*, 2020, **195**, 117076.
125 T. M. Santos, M. V. Alonso, M. Oliet, J. C. Domínguez, V. Rigual and F. Rodriguez, *Carbohydr. Polym.*, 2018, **194**, 285–293.
126 A. R. C. Morais, A. C. Mata and R. Bogel-Lukasik, *Green Chem.*, 2014, **16**, 4312–4322.
127 S. P. M. da Silva, A. R. C. Morais and R. Bogel-Lukasik, *Green Chem.*, 2014, **16**, 238–246.
128 A. Cornejo, I. Alegria-Dallo, Í. García-Yoldi, Í. Sarobe, D. Sánchez, E. Otazu, I. Funcia, M. J. Gil and V. Martínez-Merino, *Bioresour. Technol.*, 2019, **288**, 121583.
129 V. Sharma, M. L. Tsai, C. W. Chen, P. P. Sun, A. K. Patel, R. R. Singhania, P. Nargotra and C. D. Dong, *Bioresour. Technol.*, 2022, **360**, 127631.
130 N. Li, F. Meng, H. Yang, Z. Shi, P. Zhao and J. Yang, *Bioresour. Technol.*, 2022, **346**, 126639.
131 S. Arora, N. Gupta and V. Singh, *ChemSusChem*, 2021, **14**, 3953–3958.
132 Y. P. Luo, Z. Li, Y. N. Zuo, Z. S. Su and C. W. Hu, *ACS Sustainable Chem. Eng.*, 2017, **5**, 8137–8147.
133 S. Peleteiro, V. Santos and J. C. Parajó, *Carbohydr. Polym.*, 2016, **153**, 421–428.
134 M. Z. R. Mohammed, Z. W. Ng, A. Putranto, Z. Y. Kong, J. Sunarso, M. Aziz, S. H. Zein, J. Giwangkara and I. Butar, *Clean Technol. Environ. Policy*, 2023, **25**, 1551–1567.
135 G. Zang, A. Shah and C. Wan, *J. Cleaner Prod.*, 2020, **260**, 120837.
136 R. Gogar, S. Viamajala, P. A. Relue and S. Varanasi, *ACS Sustainable Chem. Eng.*, 2021, **9**, 3428–3438.
137 N. B. Appiah-Nkansah, J. Li, W. Rooney and D. Wang, *Renewable Energy*, 2019, **143**, 1121–1132.
138 R. N. Ntimbani, S. Farzad and J. F. Görgens, *Ind. Crops Prod.*, 2021, **162**, 113272.
139 R. N. Ntimbani, S. Farzad and J. F. Görgens, *Biofuels, Bioprod. Biorefin.*, 2021, **15**, 1900–1911.
140 P. Halder and K. Shah, *Bioresour. Technol.*, 2023, **371**, 128587.
141 L. C. Nhien, N. V. D. Long, S. Kim and M. Lee, *Biotechnol. Biofuels*, 2017, **10**, 81.
142 N. Viar, I. Agirre and I. Gandarias, *Chem. Eng. J.*, 2024, **480**, 147873.
143 J. Moncada, C. A. Cardona, J. C. Higuita, J. J. Vélez and F. E. López-Suarez, *Chem. Eng. Sci.*, 2016, **140**, 309–318.
144 A. Mazar, O. Ajao, M. Benali, N. Jemaa, W. Wafa Al-Dajani and M. Paleologou, *ACS Sustainable Chem. Eng.*, 2020, **8**, 17345–17358.
145 N. M. Clauser, S. Gutiérrez, M. C. Area, F. E. Felissia and M. E. Vallejos, *Biofuels, Bioprod. Biorefin.*, 2018, **12**, 997–1012.
146 V. Hernández, J. M. Romero-García, J. A. Dávila, E. Castro and C. A. Cardona, *Resour., Conserv. Recycl.*, 2014, **92**, 145–150.
147 M. Bariani, F. Cebreiros, M. Guigou and M. N. Cabrera, *Wood Sci. Technol.*, 2022, **56**, 1149–1173.

